Lab on a Chip

CRITICAL REVIEW

View Article Online
View Journal | View Issue

Cite this: *Lab Chip*, 2017, **17**, 1705

Mobile microrobots for bioengineering applications

Hakan Ceylan,[ab] Joshua Giltinan,[abc] Kristen Kozielski[a] and Metin Sitti *[abc]

Untethered micron-scale mobile robots can navigate and non-invasively perform specific tasks inside unprecedented and hard-to-reach inner human body sites and inside enclosed organ-on-a-chip microfluidic devices with live cells. They are aimed to operate robustly and safely in complex physiological environments where they will have a transforming impact in bioengineering and healthcare. Research along this line has already demonstrated significant progress, increasing attention, and high promise over the past several years. The first-generation microrobots, which could deliver therapeutics and other cargo to targeted specific body sites, have just been started to be tested inside small animals toward clinical use. Here, we review frontline advances in design, fabrication, and testing of untethered mobile microrobots for bioengineering applications. We convey the most impactful and recent strategies in actuation, mobility, sensing, and other functional capabilities of mobile microrobots, and discuss their potential advantages and drawbacks to operate inside complex, enclosed and physiologically relevant environments. We lastly draw an outlook to provide directions in the veins of more sophisticated designs and applications, considering biodegradability, immunogenicity, mobility, sensing, and possible medical interventions in complex microenvironments.

Received 18th January 2017,
Accepted 27th April 2017

DOI: 10.1039/c7lc00064b

rsc.li/loc

[a] *Physical Intelligence Department, Max Planck Institute for Intelligent Systems, 70569 Stuttgart, Germany. E-mail: sitti@is.mpg.de*
[b] *Max Planck ETH Center for Learning Systems, 70569 Stuttgart, Germany*
[c] *Department of Mechanical Engineering, Carnegie Mellon University, Pittsburgh, USA*

Introduction

Physically intelligent material systems at the sub-millimeter scale are promising for applications in various fields, such as bioengineering (*e.g.*, targeted therapeutics[1] and tissue engineering[2]), active matter (*e.g.*, programmable matter[3] and self-organizing systems[4]), and microrobotics (*e.g.*, soft

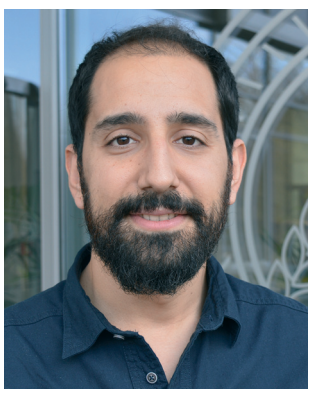

Hakan Ceylan

Hakan Ceylan has been a postdoctoral researcher in the Max Planck Institute for Intelligent Systems, Stuttgart, Germany, and currently an associated fellow of Max Planck ETH Center for Learning Systems. He received the B.Sc. degree in the Department of Molecular Biology and Genetics from Bilkent University, Ankara, Turkey, in 2010, and the Ph.D. degree in the Institute of Materials Science and Nanotechnology from National Nanotechnology Research center affiliated to Bilkent University in 2014. His research interests include intelligent materials systems, active matter, micro-scale robotics, self-assembly, bio-hybrid actuation, hierarchical material fabrication, and two-photon microprinting.

Joshua Giltinan

Joshua Giltinan received his B.S degree in Physics and Computer Science from Towson University in 2011. He is currently pursuing the Ph.D. degree in Department of Mechanical Engineering at Carnegie Mellon University, Pittsburgh, USA. In 2014, he joined the Physical Intelligence department at the Max-Planck Institute for Intelligent Systems, Stuttgart, Germany. His research interest is the fabrication and control of micro-robots and MEMS devices.

microactuators,[5] mobile microrobots[6]). Mobile functional devices at the sub-millimeter length scales afford particular advantages to pursue novel bioengineering strategies. This size regime includes the average size of a mammalian cell, the basic building unit of a tissue or organ, thereby, permitting direct access to deep, complex, and delicate body sites, such as brain, spinal cord, heart, bile duct, pancreas, and liver.[7–9] Such direct access capability potentially opens up new means of medical interventions with minimal possible tissue damage compared with the tethered catheters, endoscopes, and incision-based surgery. Further, operational resolution at sub-cellular scales would allow single cell-level manipulations with high accuracy and repeatability. In the near future, this could have tremendous applications in tissue engineering and regenerative medicine; while, in the longer term, it could revolutionize the treatment of genetic diseases by single cell protein or nucleic acid delivery.[6,10]

Use of microrobots for lab-on-a-chip devices has already proved to be a powerful tool. Handling small objects in very small fluid volumes for manipulating, moving, and reconfiguring components in 3D by means of microrobots make this route highly attractive. Assembly of 3D heterogeneous microobjects, which require orientation and positional control, would be best addressed using microrobotic assembly.[11,12] Organ-on-a-chip applications could benefit from microrobotic operations, in which complex cellular materials with 3D microscale features may need to be positioned to better recapitulate the native physiological status.[13] Additionally, preclinical characterizations of microrobots for drug release profiles and their interactions with living tissues could be tested in organ-on-a-chip platforms.

Active and targeted delivery of therapeutic cargos, such as drugs, imaging agents, and genetic materials, are the major objectives of the first-generation microrobotic systems. Active navigation inside the body to a specific target site with a controllable cargo carrier is superior to relatively limited cargo delivery and distribution efficiencies provided by current passive routes of administrations, such as intravenous delivery and local diffusion.[14] Using active, drivable carriers, it is possible to minimize systemic side effects by achieving targeted local treatment options. For example, intravenously administered interleukin-12 caused lethal systemic toxicities in a clinical trial.[15] Active delivery and controlled on-site release schemes increase the overall bioavailability of single dose administration. Sensitive cargo types, such as proteins, peptides, or nucleic acids, are better protected from degradation inside a carrier, as they otherwise have very short half-lives in serum.[16] Autonomous, real-time control over cargo release dynamics would perhaps represent the state-of-the-art of the *in situ* therapeutic and diagnostic strategy. To this end, microrobots that are able to navigate inside the human body, act intelligently in response to changing conditions, carry, deliver, and release therapeutics, and perform complicated tasks in semi- or fully autonomous manners could revolutionize many clinical practices.

The first concept of miniaturized machines for bioengineering was artistically visualized in the popular science fiction movie Fantastic Voyage (1966). In the movie, the brain clot of a nearly dying scientist had to be removed in one hour by a submarine shrunken to microscopic size and injected into his blood stream with a small crew. In view of the scaling laws, which we discuss in the

Kristen Kozielski

Kristen Kozielski received her undergraduate and Ph.D. training in the Biomedical Engineering Department at Johns Hopkins University. She completed her thesis work in the Drug Delivery and Biomaterials laboratory with Dr. Jordan Green as her thesis advisor. Her thesis work involved synthesizing nanoparticles optimized to deliver DNA, siRNA, and miRNA that could alter brain cancer behavior or kill tumor cells. Kristen is currently a postdoctoral fellow at the Max Planck Institute for Intelligent Systems, in the Physical Intelligence department. Her postdoctoral research focuses on microrobotic technologies for medical applications.

Metin Sitti

Metin Sitti received the BSc and MSc degrees in electrical and electronics engineering from Bogazici University, Istanbul, Turkey, in 1992 and 1994, respectively, and the PhD degree in electrical engineering from the University of Tokyo, Japan, in 1999. He was a research scientist at UC Berkeley during 1999–2002. He is currently a director in Max-Planck Institute for Intelligent Systems, Stuttgart, Germany and a professor at Carnegie Mellon University, Pittsburgh, USA. His research interests include mobile milli/microrobotics, advanced functional micro/nanomaterials, medical soft robotics, and programmable self-assembly. He is an IEEE Fellow. He received the SPIE Nanoengineering Pioneer Award in 2011 and NSF CAREER Award in 2005. He received many best paper and video awards in major robotics and adhesion conferences. He is the editor-in-chief of Journal of Micro-Bio Robotics.

following section, a macroscale submarine design in the microscopic dimensions is highly inefficient to operate inside human body. However, the venture of the crew has significant overlaps with premises and vision of microrobotics field, which constitute the main theme of the present review.

Here, we review frontline advances in the design and testing of microrobots for and toward bioengineering applications. In the following section, we provide a brief overview of micron-scale robotics and founding principles of this emerging field. We then make a higher-level classification of microrobots using on-board and off-board actuation, powering, and control approaches. We further subdivide each approach based on the mechanism of actuation/propulsion. We critically discuss design and operational capabilities of each type of microrobot in physiological environments, and provide potential pitfalls and parts to be optimized toward bioengineering applications (Table 1). In the final section, we provide an outlook toward more complex designs and applications. We layout future challenges and critical directions to consider for rendering intelligence to microrobotic systems.

Micron-scale robotics

A robot is by convention a reprogrammable machine with partly or fully self-contained capabilities entitled by on-board motion, perception, and learning. As a result, it can adapt to operate in complex and varying environments, and it can be programmed for different tasks. We define a microrobot in the same vein except that it has all the dimensions confined to 1 mm upper and 0.1 μm lower limits (see *Glossary* for other definitions in the context of microrobotics).[17,18] Scaling physical systems down to micron scale, the significant increase in the surface-to-volume ratio, causes surface-born interactions, such as surface tension, drag, and adhesion, to become dominant compared to volumetric bulk effects, such as mass and inertia. A substantial consequence of such scaling laws is the altering mobility methods for the microrobots.

Table 1 A brief evaluation of various microrobot designs concerning their design principles, powering and actuation schemes for generating mobility, and sensing and adaptability in the living environment

Design approach	Principal source of powering	Actuation method	Key design features for effective powering	Advantages for bioengineering applications	Major limitations
Off board (externally actuated and guided)	Magnetic fields	Rotating magnetic fields and gradient pulling	Flagellum-mimetic rigid and flexible[38] helices; cilia and sperm-mimetic undulating synthetic tails;[42] gradient pulling of magnetically active designs	Wireless powering, actuation and maneuverability; biocompatible energy source; reliable for *in vitro*, *in vivo*, and lab-on-a-chip applications	Difficulty in selective agent addressability, high cost requirements for medical instrumentation
	Acoustic fields	Acoustic radiation force and acoustic streaming	Bubble-integrated bodies; flexible tail;[84] microcannon;[87] passive particles[89]	Biocompatible energy source; both 2D and 3D assemblies can be realized; reliable for lab-on-a-chip and *in vitro* applications	*In vivo* use requires development of proper instrumentation; microrobot material composition and shape needs further investigation
	Light	Light-induced formation of thermal gradient around the microrobot	Generation of an air–liquid;[91] stable bubble encapsulation into the microrobot body[100]	Sub-micron resolution, multiple pathways for energy transfer (*e.g.*, thermal, nematic alignment); can produce traveling waves; simple selective agent addressability; reliable for lab-on-a-chip and *in vitro* applications	Limited to 2D; not applicable to *in vivo* conditions; limited workspace size; requires line of sight
On board (self-propelled)	Chemical energy	Bubble propulsion	Catalytic formation of gas bubbles by breaking down fuel in a confined reactor is ejected with high speed[102]	High swimming speed (up to 10^3 body lengths per second); robust power output	Toxic hydrogen peroxide is the main fuel source. High power output is possible with toxic catalyst like Pt. Action of Mg and Ni-driven systems elevate local pH
		Local chemical gradients formed around the microrobot	Asymmetric distribution of the catalyst, *e.g.*, Janus colloids[113]	Biocompatible fuels and catalysts, such as glucose and glucose oxidase, respectively, are possible[101]	Movement is extremely sensitive to the ionic strength; lack of long-range directional motion due to the Brownian effect
		Activation of cellular receptors	Physical attachment of live bacteria, sperm or muscle cells with synthetically engineered bodies[27]	Integrated sensing and mobility; inherently compatible with physiological fluids; comparatively high efficiency in power output	Live cells function only in delicate conditions (37 °C, 5% CO_2, nutrients *etc.*) to survive

For microrobotic swimmers in fluids, the ratio of inertial forces to the viscous drag forces, a dimensionless quantity called Reynolds number, determines the fundamental characteristics of their swimming fluid dynamics. When Reynolds number is much less than 1, viscous forces predominate inertial forces; therefore, in order for a microswimmer to propel, it has to do time-irreversible, *i.e.*, non-reciprocal, shape changes with its body.[19] As inertia plays an insignificant role in low Reynolds number, reciprocal motion does not lead to a displacement. In other words, the movement due to the forward component of the motion will be cancelled out by the backward component of the motion. In order to comply with such physical requirement, microorganisms have evolved elaborate swimming strategies, such as continuous rotation of helical bacterial flagella and non-reciprocal beating of a sperm tail and paramecium cilia. Such biological swimmers have already inspired a number of microswimmer designs, some of which are covered in the present review. Nevertheless, the size of the biological microswimmers tend to be limited by around 1 μm, because molecular diffusion predominates the advection of material to the microorganisms over the active search by swimming at the sub-micron scale.[20] As the size of the swimmer goes down to below 0.3 μm, the stochastic Brownian effect contributes to the most of the motion dynamics, thereby hindering long-range directional propulsion inside bulk fluid.[21] Below 0.1 μm, the continuum hydrodynamics does not safely apply any longer, and the effects of quantum mechanics take over. This is the domain of nanorobotics, for which the interested readers are directed to the reviews toward this direction.[22,23] Altogether, understanding the scaling forces by taking into account how physical forces are experienced by entities in the lowered dimensions is a vital aspect for the design and successful operation of microrobots.

Conventionally, a robot is made to perceive and learn by means of on-board sensing and computational capabilities, so that it can decide an appropriate response in given environmental conditions. Consequently, a prime question is how this is going to be achieved at the smaller dimensions, where such computational capabilities do not exist. Programmable physical and chemical properties of microrobots, dynamically interacting with its surrounding world, sensing, and adapting to the changes in the environment can enable robust design routes for making sophisticated systems at the microscale. In nature, organisms without brains, such as slime molds, bacteria, and plants, already use physical intelligence as the main route of making decisions and adaptations to complex and evolving conditions.[24–26] As a result, natural systems could provide a plethora of inspiration to create similarly performing artificial miniature systems based on their physical design, processing, adaptation, reconfiguration, self-organization, and control. Early attempts toward this direction have been realized as biohybrid systems where live cells are physically integrated to artificial materials to exploit their on-board integrated powering, actuation, sensing, and control capabilities.[27] This concept has recently drawn a special attention in the contexts of biohybrid microrobotics and biological soft robotics,[28] which will be discussed in detail later.

Off-board approaches for microrobots

In the off-board approach, the mobility component of a microrobot is remotely actuated, powered, and steered. Other functional components, therapeutic cargo release, could still operate in an autonomous fashion based on the local signal input. Magnetic and acoustic fields are two viable sources of actuation towards bioengineering applications of microrobots, as they are mostly compatible with the living environment by safely penetrating into deep tissues. From the practical point of view, external control also brings about a direct way of controlling the microrobot inside the body. Such approach has comparatively reduced technical challenges and therefore, it has been intensely studied, and has come closer to being applicable in *in vivo* small animal testing. However, there are still unresolved issues regarding the complicated instrumentation that comes at high costs for human scales, microrobot sensory capabilities, distributed control of multiple or swarm of microrobots, limited autonomy, and so on.

Magnetic actuation. Magnetic actuation is a prominent remote control method for powering the microrobot mobility and spatial maneuverability. In contrast to the other alternatives, such as light and chemical signals, magnetic fields are able to penetrate biological tissues and other materials safely, which make their use for bioengineering applications highly promising. Time-varying magnetic fields and their spatial gradients provide the foundation for magnetic actuation of mobile microrobots. Under the influence of field inhomogeneity, the magnetic moment of the microrobot is attracted to the region of greater magnetic flux density, and the microrobot experiences a magnetic force.[29,30] As a magnetic moment in an external magnetic field experiences a magnetic restoring torque to align it with the field, a rotating magnetic field causes an unconstrained microrobot in a fluid medium to rotate. This can be exploited to generate non-reciprocal motion, which has been shown to be necessary for moving in low Reynolds numbers.[31] Assuming the external field is invariant, the magnetic force scales with volume of the magnetic material, *i.e.*, L^3, while the equivalent force from the magnetic torque scaling with L^2. Thus, swimming by magnetic torque-induced rotation has been preferred by researchers at smaller scales, *i.e.*, *ca.* less than 100 μm, due to its higher efficiency. Regarding the safety, a static magnetic field under 8T is not considered dangerous for human medical use.[32] Nevertheless, the rate of change in gradient fields and the specific absorption rate could potentially cause tissue damage by heating. As a result, it is essential to take such safety concerns into account while optimizing the magnetic components of microrobots so as to remain within acceptable levels of magnetic field and gradient exposure set by regulatory guidelines.[33]

Using magnetic actuation, much design inspiration has so far arisen from the observation of bacteria, which use helical rotation of flexible flagella for propulsion, providing a

method to both propel forward and to change direction (Fig. 1a). While early research often yielded rigid artificial flagella, flexible DNA strands have also been shown to act as flagella for magnetic particles.[34,35] Other flexible structures have been investigated such as swimming sheets that can be controlled independently of each other[36,37] and rotating swimming microrobots with multiple flexible flagella.[38] Cellular motility structures, such as cilia and sperm-like undulations, have also served as source of inspiration for human-engineered microswimmer mobility, as well as functional microchannel coatings that provide controlled fluid motion or mixing (Fig. 1b).[39–43] Propeller-shaped microswimmers can either be human-engineered[21] or dynamically self-assembled.[44] In addition, they can have multiple modalities, alternating between swimming, rolling, and propelling, depending on the substrate and control signal.[45]

Regarding the three-dimensional (3D) maneuverability of magnetic microrobots, 5-degrees-of-freedom (DOF) control of

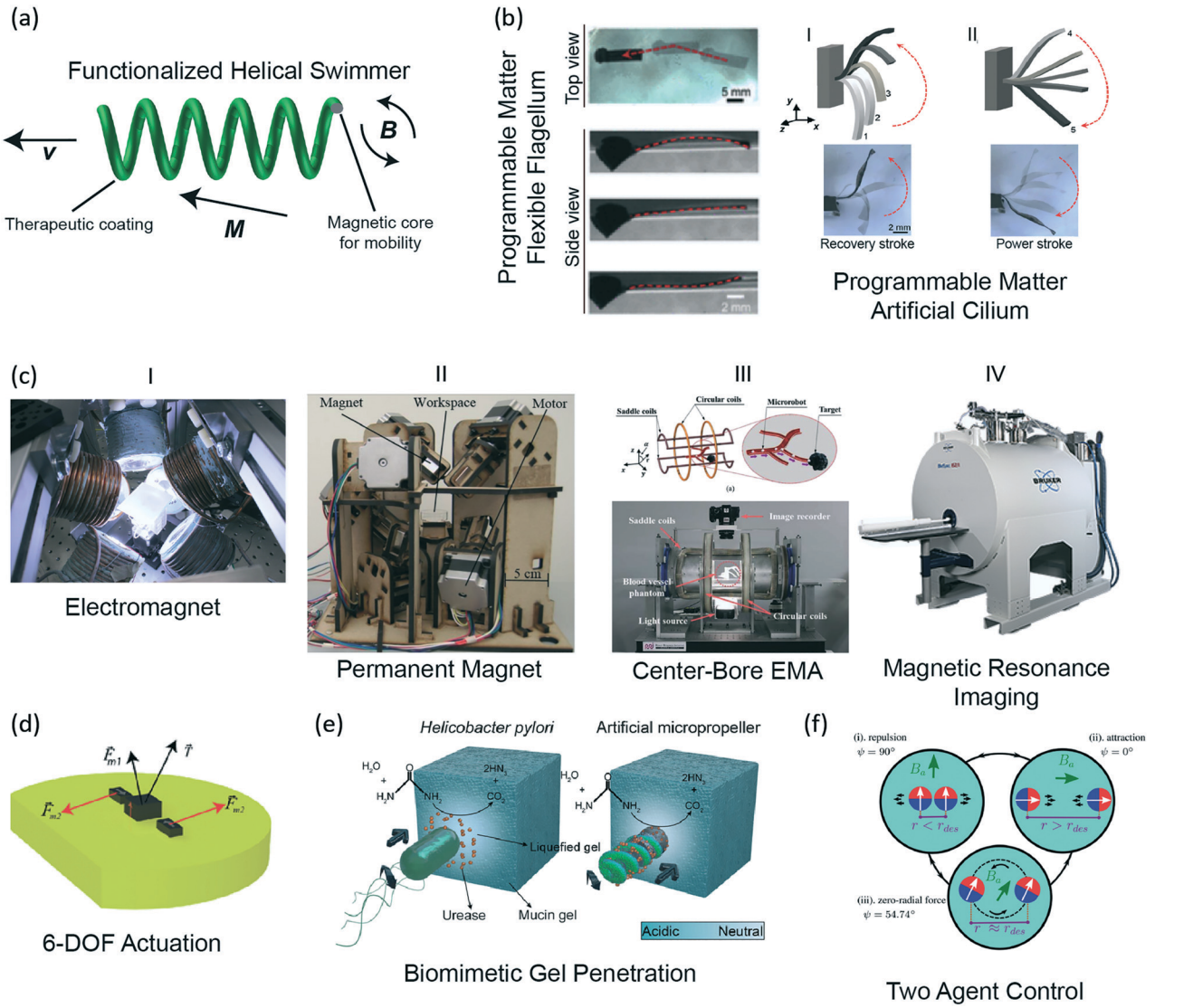

Fig. 1 Off-board magnetic actuation and powering methods for mobile microrobots. (a) Illustration of a functionalized helical swimmer, where the magnetic core is covered by a coating that can have biomedical functions, such as sensing, tissue drilling, or therapeutic drug release. (b) Programmable matter: elastomer beams, impregnated with magnetic microparticles, can be programmed to have different magnetization direction and strength locally to produce desired programmed motions, such as the undulatory motion of an artificial cilium (reprinted with permission from ref. 42. Copyright 2016 from the Proceedings of the National Academy of Sciences). (c) (i) A custom eight electromagnet coil system capable of 5- and 6-DOF control; (ii) permanent magnets mounted on stepper motors (reprinted with permission from ref. 47. Copyright 2016 from the IEEE); (iii) a four electromagnet coil system, which is capable of 3D motion control and accommodating a patient in the central bore (reprinted with permission from ref. 48. Copyright 2015 from the IEEE); (iv) a small-animal research MRI system (Bruker). (d) A body with three magnets, which create a 6-DOF controllable microrobot.[46] (e) A side-by-side illustration of an *H. pylori* bacterium and a synthetic swimming microrobot, which uses a similar mechanism to penetrate the mucin gel (reprinted with permission from ref. 53. Copyright 2015 from the American Association for the Advancement of Science). (f) The basic configurations for determining separation distance using two-agent control (reprinted with permission from ref. 66. Copyright 2017 from the Springer).

microrobots was introduced by Kummer *et al.*[8] For an arbitrary arrangement of electromagnetic coils, they showed how to solve for the forces and rigid body torques on a single magnetic microrobot (Fig. 1ci). To avoid the need for orientation feedback, it was assumed that the microrobot had a uniform magnetization, which due to the magnetic torque, would always align with the magnetic field. Thus, only the magnetic field and magnetic gradients, which create the forces, were required to achieve the 5-DOF control. However, rotation about the magnetization axis, as the vector that aligns with the field, could not be specified. By adding known, perpendicular magnetization to a magnetic microrobot, motion about all 6-DOF was shown (Fig. 1d).[46] However, as this method requires careful design and feedback, 5-DOF control is still the common method in the literature. Seeking to avoid the heat and power requirements of electromagnets, a permanent magnet-based 5-DOF control system could also provide similar path-following accuracy as an electromagnet system (Fig. 1cii).[47] 3-DOF control is also popular as many microrobots are spherical, and thus do not require any orientation control, allowing for more design freedom, such as an electromagnet configuration which incorporates a central bore to accommodate a patient (Fig. 1ciii).[48]

Gradient pulling-based magnetic microswimmers carrying plasmid DNA-loaded liposomes have been demonstrated to undertake transfection of cells for selective gene editing.[49] A microrobot coated with a 10 nm silver layer can directly disintegrate the membrane of an *E. coli* bacterium by physical contact.[50] Hyperthermia induced by microrobots is a promising method to target cancer cells, without causing damage to surrounding healthy tissue. A small rod-like microrobot, rotated at sufficiently high frequencies, can feasibly generate heat from fluid drag, but has not been shown experimentally.[51] Alternatively, magnetotactic bacteria were shown to be able to sufficiently heat to kill *Staphylococcus* bacteria in a span of 60 minutes.[52] Microrobots can also be made to penetrate through some tissues by chemical assistance, such as the *Helicobacter pylori*-inspired method of using urease activity to locally degrade gastric mucin gel (Fig. 1e).[53]

Recent works have tackled the more difficult challenge of assembling structures and transporting cargo in 3D, which cannot be based on contact-based pushing mechanisms used in 2D. Swimming or rolling microrobots induce fluid flow by their propulsion mechanism, and can use these vortices to trap objects and transport them.[54–57] Flexure-based gripping mechanisms have been shown for magnetic microrobots, where the magnitude of the magnetic field is used to control the opening and closing of the gripping arms.[58] This was shown to be highly repeatable, assembling up to 10 layers of hydrogels around a post.[12] While these untethered mechanical grippers prefer parts that match the gripper geometry, microrobots with a bubble on their surfaces could pick and place a wide range of 3D and various material parts using capillary forces.[11]

Magnetic fields have also been used for maneuverability while alternative methods serve as the source of the mobility. For example, 3D-printed microfish exhibit chemically powered propulsion while being magnetically guided.[59] Microrobots guided by magnetic fields and propelled by ultrasound were demonstrated to be simultaneously loaded with quantum dots, an anti-cancer drug, and magnetic nanoparticles.[60] An alternative propulsion method is the creation of fluid flows by the resonant oscillations of air bubbles within a fluid.[61,62] These fluid flows can additionally trap objects, and then the system can be carried by a magnetic transporter.[63,64]

Microrobot teams and swarms remain a critical research topic, because such an organization paves the way of parallel and distributed complex operations.[65] Swarm control is of particular importance as commands might be given to the whole population, subsets, individuals, or a combination of these. Control of multiple magnetic microrobots remains an ongoing topic of research, as all microrobots will receive the same global control signal. This control signal causes all microrobots to move in a coupled manner. In addition, the microrobots will either attract or repel each other due to the magnetic field gradients generated by each. By controlling the orientation of the magnets with an external field, the magnetic attraction and repulsion can be controlled to dictate the motion of the individuals (Fig. 1f).[66] Techniques to use non-uniformities in the field[67] or selective electrostatic clamps to address select individuals[68,69] have been shown, but require patterned and structured surfaces and environments. Even with these problems solved, interference of individual microrobots in a swarm yields a lower net velocity than a solitary swimmer.[70] This behavior was observed when a swarm of magnetic microrobots was driven *in vivo*, in the intra-peritoneal cavity of a mouse. However, 80 000 swimmers were required to generate a sufficient fluorescence signal to track and when coupled with the complex biological fluid medium, the mean speed decreased to 6.8 $\mu m\ s^{-1}$, roughly half of the length of the microrobot body per second.[70]

While swarm microrobotics is promising for minimally invasive surgery, research in the functionality of individual micororobots for *in vivo* use has progressed. An artificial arterial thromboembolism was penetrated inside a live porcine model by a centimeter long microrobot using fluoroscopic imaging for position control.[71] Recent *in vitro* efforts have focused on improving functionality of microrobots that will eventually operate inside the body. Intra-ocular surgery is still on track to be the first use of a medical microrobot in humans, as a camera above the patient will allow for fast, non-invasive feedback of the microrobot position. Recent advancements have enhanced the mobility of microrobots in vitreous fluid and tested online measuring of the viscoelastic properties of the vitreous, vital for control optimization.[9,72]

The electromagnet coil systems discussed are often customized for *in vitro* research. To transition to clinical *in vivo* applications, commercial systems must either be developed or adapted from existing technologies. A magnetic resonance

imaging (MRI) device is a diagnostic tool that is utilized by most hospitals and adapting this technology could provide an affordable therapeutic modality for many clinical settings. An MRI device can both localize and actuate a microrobot toward their clinical use (Fig. 1civ). To this end, the existing MRI devices are promising, but advances in the state-of-the-art are limited due to both the high static magnetic field and the high cost-of-entry for research. Static, multi-DOF MR-compatible devices have been developed, but mobile device control remains in its infancy.[73] Recent work has been able to operate such a microrobot inside a phantom with over 100 Hz feedback by limiting imaging to the direction of the applied gradients, so that all imaging sequences will yield propulsive force.[74] A mobile injection system has been developed in use of an MRI by using the transfer of magnetic energy in a Gauss gun configuration.[75] Magnetic particles can be tracked in an MRI to visualize blood vessels that are smaller than the current resolution limits of an MRI.[76] If the microrobot is non-magnetic, ongoing research is increasingly miniaturizing electromagnetic coils to be placed on-board a device for visualization by the MRI, though on-board miniaturized power remains an ongoing challenge.[77] If the object is magnetic, a new technique, dipole field navigation, was developed for tracking and actuation in an MRI. This technique allows for actuation that requires large spatial gradients, provided by a placing a magnetic sphere outside of the patient. By placing the magnet near the targeted microrobot, actuation can be achieved, and by moving the sphere with the MRI gradient coils, the MRI can automatically image and actuate the microrobot; however, optimization and *in vivo* validation and testing remain as future works.[78,79]

Acoustic actuation. Acoustic fields are another compelling source of remotely powering the microrobot mobility in controlled directions. As a technology, it is an emerging and promising field for off-board propulsion and manipulation of microrobots, while its functional design and application in a biological setting is currently insufficient and requires future developments. The physical effects of acoustic fields are mostly exploited in the forms of acoustic radiation force and acoustic streaming. Acoustic radiation force can be generated by a standing wave, which is created when a sound wave reflects back and forth in a resonator, in a biologically safe way. This creates a hydrodynamic drag force in a fluid for driving microobjects to the sound pressure nodes and antinodes, which are minimum and maximum amplitude points, respectively.[80,81] In this actuation scheme, the direction of motion can be predicted and dynamically altered by the corresponding wave functions. As a result, this method could be quite effective in controlling the global mobility of multiple microobjects to accumulate them in the target sites. For tissue engineering applications, in particular, this method is appealing to organize cells in 2D and 3D patterns as dense aggregates.[80–82] It is typically ineffective for addressing individual structures, as the acoustic fields do not have selectivity to the manipulated objects. However, application of acoustic radiation force fields in an oscillatory fashion has recently been introduced for selective addressability. In this system, oscillating bubbles trapped within microswimmer bodies generated sufficient thrust, so using a group of microswimmers each with a unique bubble size, selective actuation of a single microswimmer from among the group was shown to be possible (Fig. 2a).[62,83]

In the context of *in vivo* applications, the standing wave method is limited, because standing waves cannot be established in the human body in a predictable manner. For *in vivo* efficient propulsion, traveling wave-mediated mobility is the most advantageous strategy. In this context, an acoustically activated flagellum was recently shown to propel an artificial microswimmer through an aqueous solution by small amplitude oscillation of the tail in the presence of travelling acoustic waves (Fig. 2b).[84] Acoustically responsive, sperm-shaped microswimmers can also be fabricated *in situ* within a microchannel and therein actuated *via* flagella oscillation.[85] On the other hand, this method falls short for size scalability and maneuverability, which remain as the major improvements in the future.

Acoustic radiation force can also be generated by focusing an ultrasonic beam to physically trap an individual or a group of microobjects.[86] The trapped microobject can then be transferred by moving the ultrasonic transducer that generates the ultrasound. However, strong ultrasound at the focal point may cause a high temperature rise resulting in tissue damage. A noteworthy study turned this local energy buildup into advantage and proposed a potential method of drug delivery. Focused ultrasound pulse vaporized perfluorocarbon emulsion within a microcannon that resulted in rapid ejection of microparticles (Fig. 2c).[87] During the ejection, the speed of microparticles reached exceptionally high speeds of a few meters per second. Acoustic streaming can also generate directional propulsion force in fluids. Ultrasound actuation of a simple structure consisting of an array of comb-like cavities with trapped air bubbles oscillating at the resonant frequency of microbubbles propels the structure in the direction opposite to the acoustic streaming.[88]

Holographic acoustic elements have recently been introduced as a strong tool for complex manipulation of microobjects wirelessly. A remarkably simple method introduced by Fischer *et al.* demonstrated a 3D-printed surface profile used to encode the acoustic phases of the desired wavefront for enabling intricate particle patterning and trajectory control (Fig. 2d).[89]

Photo (optical) actuation. A thermal gradient across an air–liquid interface will induce fluid flow in the direction of the cooler region, due to the temperature dependent nature of surface tension. In opto-thermocapillary manipulation, the thermal gradient is generated by a focused light source, and microbubbles are manipulated as they host the air–liquid interface. In this actuation scheme, maneuverability can easily be controlled by moving the light source, thereby reforming the thermal gradient in a steady state manner. A major drawback of this, however, is that currently these

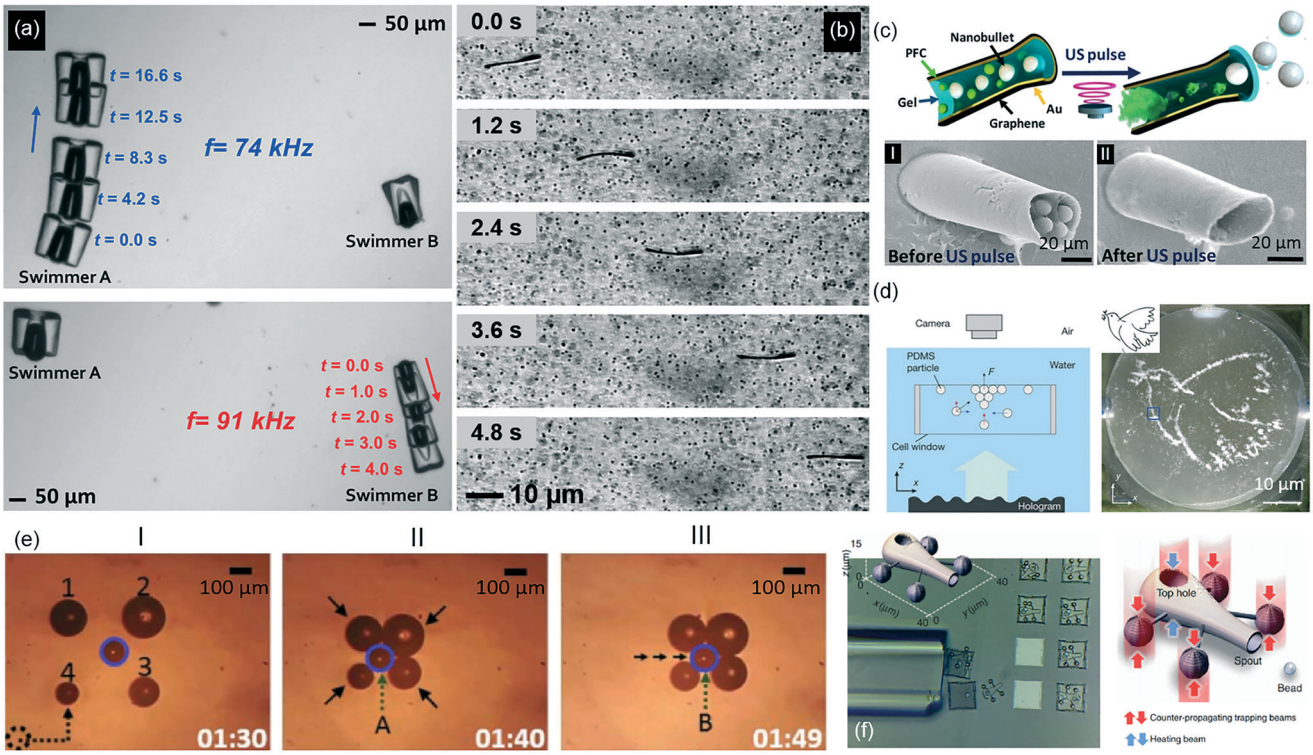

Fig. 2 Off-board acoustic and optical actuation, powering, and control strategies for microrobots. (a) Low-power acoustic field driven oscillatory motion of a bubble enables directional motion in water. Two microswimmers with bubbles of different size enable independent control of each body (reprinted with permission from ref. 83. Copyright 2015 from Nature Publishing Group). (b) A flexible tail attached to a rigid body is actuated by travelling acoustic waves that result in directional motion (reprinted with permission from ref. 84. Copyright 2016 from the American Chemical Society). (c) Ultrasound triggered high-speed ejection of microparticle cargo from cannon-like microholes (reprinted with permission from ref. 87. Copyright 2016 from the American Chemical Society). (d) Hologram-based patterning of acoustic waves drives the assembly of microparticles into predictable reconstructions in 3D (reprinted with permission from ref. 89. Copyright 2016 from Nature Publishing Group). (e) The automated simultaneous manipulation of four heterogeneous bubbles by thermocapillary flow enables the bubbles to surround and transport a microobject (reprinted with permission from ref. 92. Copyright 2016 from the IEEE). (f) A light controlled microrobot with a particle ejecting function. By illuminating the top hole, which has a thin layer of gold for heat transduction, the resulting thermocapillary flow ejects a bead (reprinted with permission from ref. 100. Copyright 2016 from Nature Publishing Group).

setups require special substrates to transduce light into heat, and have only been demonstrated in 2D. Readers interested in recent fundamental science of thermocapillarity are referred to the literature.[90] Toward their application, it has been recently shown that a large number of bubbles can be generated and independently manipulated by using a liquid crystal device, which can modulate a laser wavefront into multiple outputs.[91] This technique has been demonstrated by an automated system to trap microobjects by surrounding them with bubbles and then pushing the object to a desired position (Fig. 2e).[92] Thermocapillary flow is also applicable to a liquid droplet in air. However, if the substrate were hydrophobic, the droplet would move slowly. It was shown that a lubricant layer between the droplet and substrate can increase the velocity of the flow by a factor of five.[93] A hybrid micromotor can use opto-thermal and chemical responses to propel through a fluid, and act as a rudimentary "logic circuit", due to its selective responses to both light and chemicals.[94]

Light can also directly propel untethered microdevices. A soft device comprised of a liquid crystal elastomer exhibits peristaltic motion under a modulated travelling light wave.[95] Similarly, a liquid crystalline microrobot can crawl on surfaces by contracting when heating above 100 °C and expanding with directional friction due to asymmetric legs.[96] This can be scaled up to a few millimeters, and by patterning the liquid crystal elastomer, the contraction can produce travelling waves in the structures, allowing the microrobot to move by propelling the wave down the length of the microrobot.[97] Optical trapping, using a laser source to hold the position of a microparticle in 3D, was developed over 30 years ago. However it cannot directly manipulate objects greater than a few microns, and has been extensively covered in the literature, though novel bioengineering uses are being developed.[98] If the particle is engineered asymmetrically, the beam does not have to be directional or focused, instead the thermophoretic effect propels the particle in *a* direction depending on the particle design and light wavelength.[99] Recently a mobile microrobot with a syringe function was developed by exploiting four optical traps manipulating four handles on the microrobot. In the center, they fabricated a metal layer that could generate bubbles and

thus thermocapillary convection flow, which is used to capture and "inject" microobjects (Fig. 2f).[100] Optical trapping can also bend an air–liquid interface, and the resulting stored elastic energy is able to propel a bubble like a catapult when released.[101]

On-board approaches for microrobots

In the on-board approach, a microrobot is self-contained with all the components necessary to move, sense, and operate in a manner independent from an external intervention. Additionally, dynamic feedback and control mechanisms regulating the interactions among functional components are central to achieve intelligent performance. To power these actions, the microrobot should harness chemical energy available in its microenvironment using its physical and programmed intelligence. As a result, the complexity of such fully self-contained autonomous microrobots is greater than that of a microrobot designed by the off-board approach.

Self-propelled chemical microrobots. In self-propelled chemical microrobots, all components are typically synthetic, and the microrobot uses available chemical energy present in the microenvironment, *e.g.*, a fuel, to power the mobility, sensing, and other functional capabilities. The source of the input energy could be either organic, *e.g.*, glucose, or inorganic, *e.g.*, hydrogen peroxide, depending on the type of the catalyst used to process it. Most of the efforts along this line have so far focused on developing various types of micromotors, which can undertake the chemical conversion to release the energy stored in the chemical bonds, and then convert this free energy to do work in the form of directional motion. As inertia plays a negligible role for the propulsion in the low Reynolds regime, the chemical conversion needs to be continuous in order to sustain motion. Besides, the microrobot has to break the time-reversible symmetry to be able to move. Considering these design aspects, strategies towards making chemically powered directional motion are concentrated around two approaches. First, continuous bubble formation in the confined cavity of a micromotor and its subsequent jet-like expulsion from a nozzle drives long-range directional motion (up to 10^3 body lengths per second) in 3D.[102] In the case of hydrogen peroxide fuel, for example, it undergoes a disproportionation reaction by the catalytic activity of platinum that yields water and gaseous oxygen, which constitutes the source of the bubble. The typical size of bubble-propelled micromotors range on the orders of 10^0–10^2 μm while self-assembled, polymeric stomatocyte around 0.3 μm represents the smallest example using this mechanism for propulsion.[103] In the second approach, local chemical gradients formed around the micromotor generate a self-phoretic thrust force. Mobility using this small force is possible only for micromotors smaller than 3 μm down to the molecular scale.[104–106] In the molecular scale, the catalytic activity of enzymes results in enhanced self-diffusion.[107,108] Even though the chemical reactions occurring at the swimmer-medium interface provide strong phenomenological insight, the true physics behind the propulsion is still under intense debate for both approaches.[108–113]

Bubble-propelled microswimmers are mainly fabricated in tubular shapes, which contain the catalytic material in the inner layer. This enables accumulation and accelerated ejection of the bubbles in well-confined and controlled reactor (Fig. 3a).[114] As the gas accumulates and the internal gas pressure grows up, the resulting bubble accelerates towards one end to be ejected from an opening to the outside environment. It was suggested that the momentum change during the bubble ejection plays a critical role to drive the motion in the opposite direction.[109,114] Tuning the magnitude of the momentum change by external stimuli such as temperature, light, and ultrasound modulated the microswimmer speed in a dynamic way. For example, ultrasound induced disruption of normal bubble evolution and ejection was an interesting method for microswimmer speed control. By this means, it was possible to achieve very fast changes in the micromotor speed in less than 0.1 s as well as reproducible on/off control (Fig. 3b).[115] Another strategy toward this direction was folding and unfolding of the rolled-up polymer-platinum tubes by means of temperature changes, which resulted in speed control between 100–250 μm s^{-1} (Fig. 3c).[116] In a recent study, temperature-sensitive polymer brushes were chemically grown onto the bubble-propelled stomatocytes, where the change in the temperature narrowed or enlarged the opening into the catalytic site. Control over the catalytic turnover rate by tuning the access to hydrogen peroxide fuel regulated thrust force and the resulting swimming speed.[117] UV irradiation was used in another study to activate tubular micromotors made of TiO_2 that propel themselves in the presence of hydrogen peroxide by generating oxygen bubbles.[118] The intensity of UV light allowed a facile speed control between 50–250 μm s^{-1} with 0.2 s response time. However, these methods are external, off-board approaches, and no on-board mechanism has been reported for self-controlled catalytic activity of the micromotors to control the swimming speed so far.

The movement of bubble-propelled microswimmers typically follows random trajectories in 3D. Their directional control to date was accomplished by wireless external control, such as magnetic, electric, and acoustic fields, in a way similar to that of off-board approach.[119] An autonomous strategy was only recently demonstrated for the first time in the form of chemotaxis, where chemotherapeutic drug doxorubicin-loaded 0.3 μm swimmers move along a hydrogen peroxide concentration gradient toward higher fuel concentration.[120]

While bubble-propelled microswimmers can robustly operate in high ionic media, the termination of motion may be desired, *e.g.*, when the microswimmers reach a target goal. This can be accomplished by the irreversible inhibition of the catalyst. For example, the presence of sulfhydryl groups in the environment is detrimental to the function of platinum mounted micromotors. Otherwise, a typical bubble-propelled microswimmer has sufficiently long lifetime,

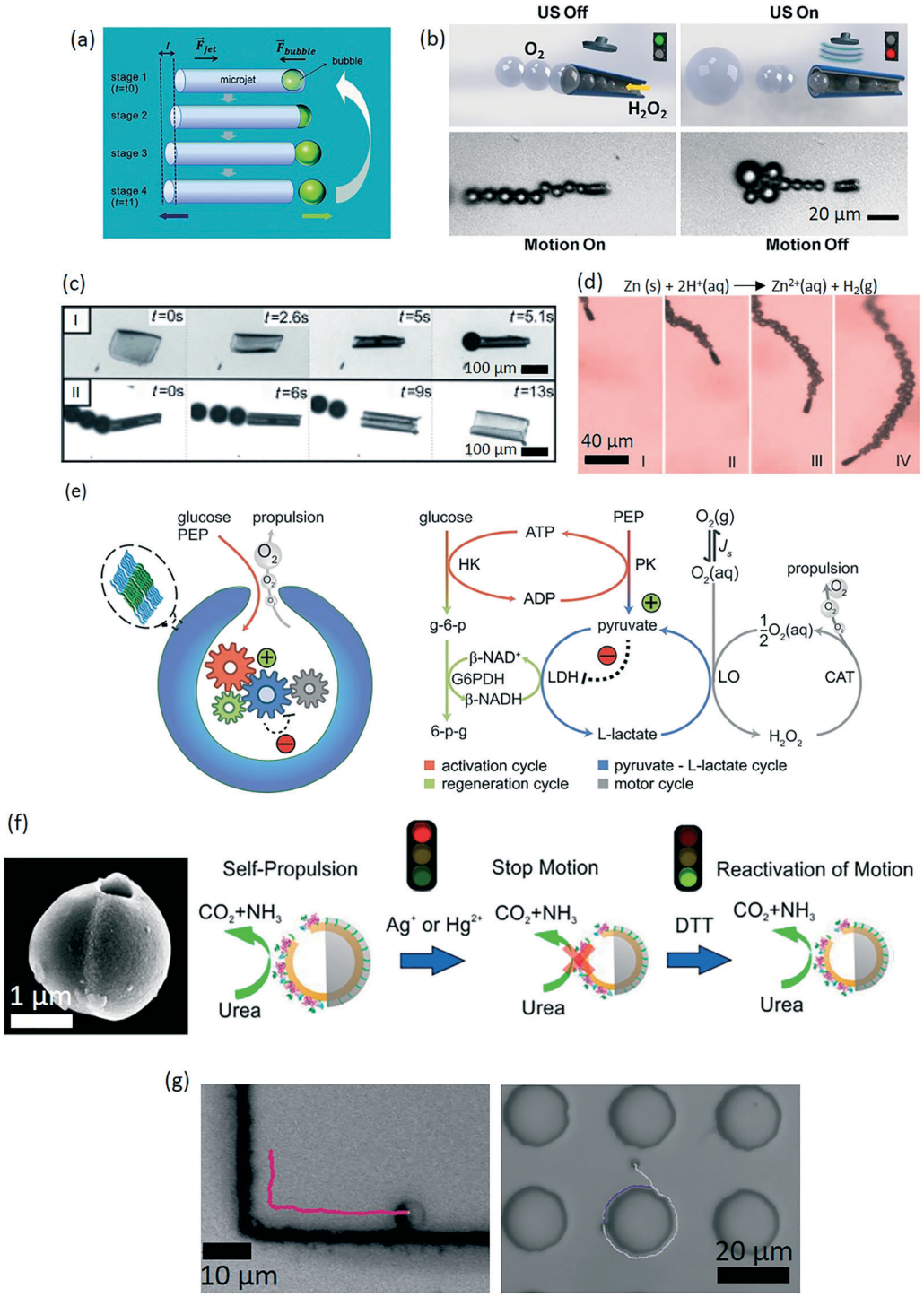

Fig. 3 Chemically powered microrobots. (a) A schematic diagram of a bubble-propelled microswimmer motion step. The bubble makes a cyclic and asymmetric change from "bubble inside" into "detached bubble", which causes the motion of the microswimmer (reprinted with permission from ref. 114. Copyright 2011 from the Royal Society of Chemistry). (b) Speed modulation of hydrogen peroxide-based, bubble-propelled microswimmers by ultrasound. Application of the ultrasound disrupts the bubble evolution and hence reducing the swimming speed (reprinted with permission from ref. 115. Copyright 2014 from the American Society of Chemistry). (c) Maturation of effective bubbles for motion depends on the geometry of the film. The visible oxygen bubbles are formed only in the cavity of a tube. (I) Folding of stimuli-responsive films by cooling below 28 °C. (II) Unfolding by warming up with stopping of bubbles (reprinted with permission from ref. 116. Copyright 2014 from the John Wiley & Sons, Inc.). (d) Time-lapse images of zinc-based microrobots in gastric acid at 37 °C (1 s intervals, I–IV) (reprinted with permission from ref. 125. Copyright 2015 from the American Society of Chemistry). (e) Development of a rationally designed metabolic network for temporally sustained autonomous movement at constant speed (reprinted with permission from ref. 128. Copyright 2016 from the American Society of Chemistry). (f) Velocity control of a Janus micromotor by manipulating the enzymatic activity of urease (reprinted with permission from ref. 131. Copyright 2016 from the American Society of Chemistry). (g) Long-range directional motion of colloidal Janus particles, guided along prescribed topographic pathways (reprinted with permission from ref. 136. Copyright 2016 from Nature Publishing Group).

allowing continuous operations for weeks without loss of performance.[121]

Load and transport of cargo mounted on the body of bubble-propelled micromotors have already been demonstrated toward their use in bioengineering applications.[102,119] Concerning the fuel type, hydrogen peroxide has been the major fuel type for both bubble-propelled and self-phoretic swimmers, mostly because it provides simple and reproducible conditions to study the basic mechanisms of swimming. For the bioengineering applications, however, it is highly corrosive and thus a major problem. Similarly, hydrazine, strong acids or bases, and bromine/iodine fuels require conditions that are unlikely to be biocompatible. An important direction for self-propelled chemical microrobots is therefore to discover new catalysts that utilize biologically available or biocompatible chemicals. Besides, most of the inorganic catalysts, such as platinum, pose a safety risk in the biological environment. In this regard, enzymes have been recently regarded as biocompatible alternative of inorganic catalysts. To this end, platinum was substituted with catalase, which performs similarly rapid peroxide decomposition for bubble-driven motion.[103,122] Alternatively, water-powered magnesium and zinc-based microrobots represent recent examples toward biocompatible application of bubble-propelled microswimmers.[123] In these cases, magnesium and zinc are consumed by reacting with water to produce magnesium hydroxide and zinc hydroxide, respectively, along with the evolved hydrogen gas, which forms bubbles to drive motion. In this regard, coating magnesium particles with a red blood cell membrane was demonstrated to detoxify serum-like solution from protein toxins.[124] A potential safety risk of this system, however, is rapid elevation of the local pH due to magnesium hydroxide buildup. Nevertheless, depending on the specific body site, this may be an accepted, or even advantageous, route of powering. For example, microrobots based on the magnesium- and zinc-powered micromotors could be well suited for operations in the acidic gastrointestinal tract. To this end, autonomous motion of zinc-based micromotor was demonstrated for the first time *in vivo* in the stomach of a live mouse (Fig. 3d).[125] In the stomach acid, self-propulsion of the micromotors led to increased binding to the stomach wall, and improved retention of the payload in the stomach compared to the passive diffusion. One key advantage of using zinc or magnesium is that the micromotor is self-destructive meaning that it does not leave a toxic residue in the body.[126] In the case of intestinal delivery, oral administration of the microrobots is the main route. In order not to prematurely consume the propulsion source in the gastric acid, the micromotors could be shielded by enteric coating, which is insensitive to the pH of gastric acid (pH 1–3) whereas it dissolves in the intestinal fluid (pH 6–7) to expose the micromotors to start the movement.[127] It is also noteworthy to add that in contrast to the catalytic approach, consumption of magnesium results in short-lived microrobots, endangering the completion of the operation before running out of its magnesium.

Mobility of the bubble-propelled microswimmers is strongly dependent on the accessible fuel concentration in the immediate microenvironment. Given the fuel amount, the mobility of the microswimmer gradually diminishes as the fuel is consumed, and propulsion ceases once the fuel consumption is complete. To maintain the speed at a constant speed over time, a far-from-equilibrium enzymatic network that actively regulates the fuel supply was demonstrated (Fig. 3e).[128]

Chemically powered self-phoretic microswimmer designs have been established around making colloidal micro- and nanoparticles with asymmetric distribution of the catalyst.[104–106] Asymmetric catalyst creates an asymmetric decomposition of the reactants and formation of products, facilitating self-generated, local chemical gradients that create thrust forces. The resulting microswimmer speed is also proportional to the catalytic turnover rate, and hence the effective surface area of the catalyst.[129] On the other hand, a long-range directional motion in bulk fluid using this method is not possible due to strong interference of stochastic Brownian effects. For this reason, such systems are also called as active Brownian particles that exhibit an interplay between random fluctuations and short-range directional swimming, thereby resulting in enhanced effective diffusion coefficient.[113] This is an interesting behavior dominated by directed motion on short time scales and by an enhanced random diffusion in long time scales.[130] As a result, there is a strong need to understand the behavior of such micromotors in real-life environments, where such randomness could play a particularly useful role to execute certain bioengineering tasks, such as real-time health monitoring and emergency intervention if need be. Nevertheless, in order for self-phoretic particles to move, the ionic strength and viscosity of the fluid are very critical, which puts a major challenge for the current version of the self-phoretic microswimmers in the ionically rich living environment. To control motion, an on/off control mechanism was shown in the enzyme-driven microswimmers, which was achieved by reversibly inhibiting the enzymatic activity (Fig. 3f).[131] For maneuverability, external magnetic guidance[131,132] and gravitaxis[133] were demonstrated.

When self-phoretic chemical microswimmers are around a solid boundary, interesting motion behavior can be observed. The microswimmers can sense the presence of the boundary through chemical and hydrodynamic interactions, and respond to it by exhibiting reflection, steady sliding, and hovering effects.[134,135] An attraction potential between the particle and the wall exists so that the particle cannot escape due to rotational diffusion. Using this, self-phoretic micromotors could be guided along prescribed paths on microstructures (Fig. 3g).[136]

Enzymatic catalysis has broader applicability in self-phoretic swimmers, where more biocompatible fuel sources, such as glucose and urea, were decomposed by the catalytic activity of glucose oxidase and catalase enzymes, respectively.[105,131,132] Nevertheless, an important drawback of

enzyme catalysis is the short lifetime of the proteins that may fall short to realize the desired outcome with the microswimmer.

Biohybrid cell-driven microrobots. In the previous sections, the components of microrobots, such as actuation, motility, and other functional units are made from synthetic materials, such as polymers, magnetic particles, and metals. These systems have so far lacked an integrated intercomponential communication and control, which requires more rigorous out-of-the-box thinking. In nature, microorganisms, such as bacteria, spermatozoa, and muscle cells, in the size range of 1–20 μm, have evolved over millions of years to operate in highly robust and adaptive manners. Their onboard machineries are continuously converting the available chemical energy in their surroundings into mechanical work, and can regulate its power output by responding to forces, mechanical strain, and chemicals in their environment through highly sophisticated control pathways. In the biohybrid approach, single cells or a tissue/film composed of such cells are physically incorporated with synthetic materials to exploit the powering and sensing capabilities of the cells toward creating complex functional microrobots.[6,27,137] Cells use active mechanical motion to propel with high energy efficiency, instead of self-generated chemical or temperature gradients. Hybridization of animate and inanimate components in creative designs may enable complex microrobotic tasks to be carried out fully autonomously.[138] This level of complexity may further enable parallel and distributed operations to be accomplished by teams or swarms of biohybrid microrobots. In addition, despite to all-synthetic systems, biohybrid systems are already adapted to work in physiological fluids. In this section, we discuss the recent advances of engineering biohybrid microrobots, and strategies toward their biomedical applications.

Flagellated bacteria species and spermatozoa are motile microorganisms that can generate thrust forces on the orders of 10^{-3} and 10^{-1} nN, respectively.[139,140] This power is sufficient to actuate the movement of micron-scale particles (Fig. 4a).[137] However, as the movement of each cell is stochastic in nature, directionally controlled actuation presents a challenge. In addition, as most bacteria-driven biohybrid particles tend to be functionalized with more than one cell, opposing forces can further limit the speed or directional control of the robot.[141] In this regard, one strategy to direct biohybrid robot swimming is to use the cells' innate environmental responses to signals such as pH, temperature, chemicals, or light.[142–144] Remote magnetic fields can also be used to steer cell-driven biohybrid microrobots by integrating to them magnetic micro/nanoscale particles or thin films.[145–147] Anisotropic cell patterning strategies have also arisen that bias the movement of the biohybrid robots in the direction opposite to the cell functionalization.[141]

Although single bacterium movement in response to environmental cues is well characterized, the coordinated movement of several bacteria attached to a particle has only recently been described. To this end, multiple *S. marcescens*-functionalized microparticles were demonstrated to conduct uni- and bi-directional pH-taxis towards neutral pH environments (Fig. 4b).[148] Moreover, a microrobot model was developed in this work, which was able to isolate swimming direction and speed bias as the major factors that contributed to the pH-taxis behavior. Because a common cellular signaling pathway is believed to be responsible for different bacterial tactic responses,[149] it is possible that such models could be used to optimize the directional control of chemotactic or thermotactic bacteriobots as well.

Cancer therapies by bacteria-driven microrobots have recently emerged with promising results. Tumor-targeting bacteria *Salmonella typhimurium (S. typhimurium)* was attached *via* biotin-streptavidin linkers to nanoliposomes loaded with chemotherapeutic paclitaxel.[150] *In vitro* co-culture experiments demonstrated that the bacteria-based microrobots selectively migrated towards a murine mammary carcinoma line (4T1), rather than toward healthy human fibroblasts (NIH/3T3), and they led to paclitaxel-mediated 4T1 cell killing. Although this work was not *in vivo*, earlier works with free *S. typhimurium* showed promising cancer-selective tissue localization,[151] suggesting the promise of employing this strategy in *in vivo* studies in the future. Magneto- and aerotactic bacteria *Magnetococcus marinus* strain MC-1 (MC-1) was recently used as an *in vivo* active drug carrier *via* cell surface functionalization with drug-loaded nanoliposomes (Fig. 4c).[152] In the direction of the constant magnetic field of an MRI system, the active carriers were steered toward a subcutaneous human colorectal tumor (HCT116) region implanted inside a rat. Magnetic guidance enabled millimeter-scale tumor penetration, while the bacteria's aerotactic behavior enabled micron-scale localization into the hypoxic regions of the tumor.

Because microscale fabrication and control are challenging, particularly with biological components, further optimization of biohybrid swimmers is necessary for their realization in applications, such as drug delivery or diagnostic devices. Stochastic bacterial motion on the surface of bacteria-driven microrobots can be directionally controlled using steering at the particle level. *Serratia marcescens* (*S. marcescens*) bacteria-driven magnetic microparticles could be steered using remote magnetic fields.[145] Since a magnetic field was employed to apply magnetic torque on the robot, rather than a magnetic gradient to apply magnetic force (*i.e.* pulling), the driving field strength could be kept low (on the order of a few or tens of mT). Using such method, a bovine sperm-driven microrobot was steered using closed-loop control for its precise navigation control.[153] The sperm-driven microrobot consisted of a conical tube made of magnetic thin film, which was used to capture a swimming sperm cell inside, such that its tail remained free and was able to provide propulsion.[154] By applying low magnetic fields (1.4 mT), the robot was steered at speeds of 25 ± 10 μm s^{-1} to a target position with a 90 ± 40 μm precision. Also, spinning micron scale helices coated with magnetic thin films were used to trap and transport immotile sperm cells in an *in vitro*

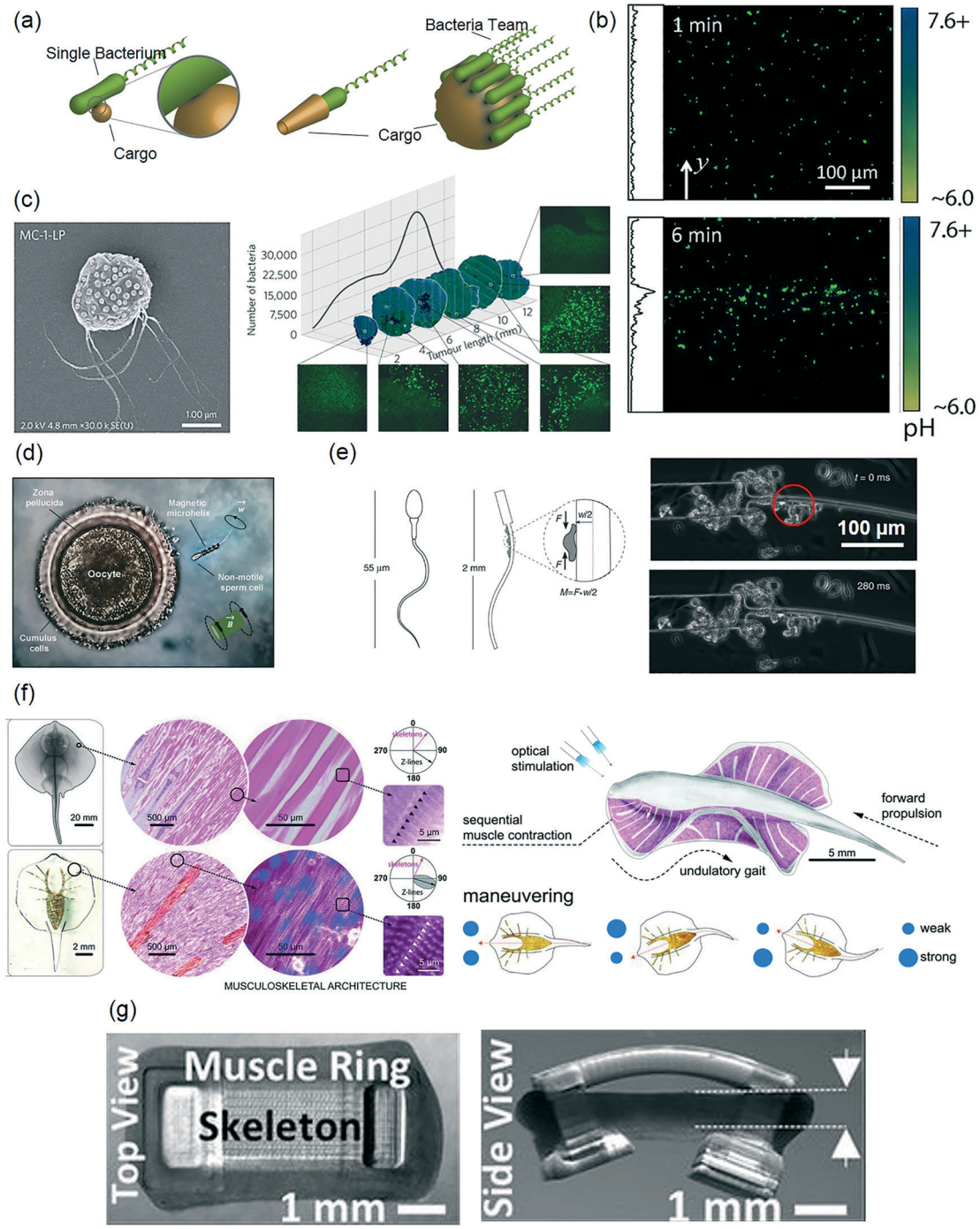

Fig. 4 Biohybrid microrobot design and application strategies for bioengineering applications. (a) Conceptual designs of bacteriobots by attaching motile bacteria to synthetic drug cargos (reprinted with permission from ref. 137. Copyright 2016 from Elsevier). (b) Fluorescent micrographs of bacteriobots demonstrate pH-triggered accumulation over time, indicating a uniquely coupled motion and sensing capability of biohybrid designs (reprinted with permission from ref. 148. Copyright 2015 from Nature Publishing Group). (c) Left: Magneto- and aero-tactic bacteria *Magnetococcus marinus* strain used to make a nanoliposome-bacteria biohybrid construct to target mouse tumor. Right: Transverse tumor sections actively populated by the bacteria (reprinted with permission from ref. 152. Copyright 2016 from Nature Publishing Group). (d) An immotile sperm is captured by a remotely controlled magnetic helix and delivered to the oocyte for fertilization (reprinted with permission from ref. 1. Copyright 2016 from the American Chemical Society). (e) An elastic 1D filament with a rigid head and a compliant tail, and a small, single cluster of muscle cells generating power to create asymmetric motion for swimming (reprinted with permission from ref. 160. Copyright 2014 from Nature Publishing Group). (f) Musculoskeletal meso- and micro-architecture of a skate, *L. erinacea* is replicated in a 2D tissue-engineered ray. Upon optical stimulation, the tissue-engineered ray induces sequential muscle activation *via* serpentine-patterned muscle tissues, generates undulatory locomotion, and sustains steady forward swimming. It changes direction by generating asymmetric undulating motion between left and right fins, modulated by light pulse frequency (reprinted with permission from ref. 158. Copyright 2016 from the American Association for the Advancement of Science). (g) Optogenetic 3D muscle ring-powered biobots (reprinted with permission from ref. 157. Copyright 2016 from the National Academy of Sciences of the U.S.A.).

fertilization experiment (Fig. 4d).[1] Single sperm cells could also be released from swimming microtubular structures using remote temperature control.[155] Finally, electric fields can also be used to steer bacteria-driven microswimmers.[156]

Unlike bacteria and spermatozoa, muscle cells do not have a specialized swimming component. Skeletal and cardiac muscle cells contract to generate a directional tension on the order of 10^3–10^5 nN in magnitude, in response to an artificial excitation stimulus, such as, chemicals or electric field.[27] However, these stimuli are invasive and not practically useful toward bioengineering applications. To this end, recently, both skeletal and cardiac muscle cells were genetically engineered for optogenetic light stimulation, and were successfully used in biohybrid soft robotic constructs (Fig. 4f and g).[157–159] As the light-mediated excitation is also spatially well controlled, this method further enabled a steering control by local contractions and maneuverability (Fig. 4g).[158] Coupled with the actuation frequency, the magnitude and frequency (1–5 Hz) of muscle cell contraction was repeatable and controllable. This property opened up a design window for muscle-based microrobots, or myobots, in which the spatial organization of the cells on the substrate enables transferring of the contraction force, and hence the bending of construct in a predictable manner. In this regard, 1D biohybrid constructs were shown to be actuated by only a few muscle cells (Fig. 4e).[160,161] This actuation could generate sufficient force to make it swim in low Reynolds numbers.[160] In 2D, careful spatial decoration of muscle cells on a flexible surface enables programmable control of the cell contraction force in both time and space domains, thus allowing for complex designs.[158] In 3D, organization of cells is a lot less accurate in terms of force distribution. Nonetheless, a 3D-printed asymmetric shape hydrogel was shown to be powered by skeletal muscle cells that resulted in a stick slip locomotion.[162] In this fabrication scheme, cells were packed in high densities embedded in a supportive hydrogel matrix to maintain the overall integrity. Cell-embedded hydrogel could be molded in particular shapes, which was then incorporated to a synthetic polymer for predetermined actuation. In this way, it was possible to generate 300 μN active tension in the final construct.[157] In addition to the inefficiency of the cell placement in 3D, another major limitation for a 3D construct is the lack of transport of nutrients through high cell densities in a sustainable manner.

Outlook

Microrobotics has sparked a significant excitement in recent years, where the proposed microrobots are aimed to have abilities of sensing, making decisions, and performing specific functions in physiologically, *i.e.*, biochemically, changing and complex environments. In this direction, they possess high potential for a range of bioengineering applications, including therapeutic delivery, tissue engineering, microsurgery, and biosensing. Their microscopic size makes them unrivalled for accessing into small, highly confined and delicate body sites, where conventional medical devices fall short without an invasive intervention. Realization of such applications, however, first, requires proper attention towards achieving improved material biocompatibility, lowering potential immunogenic reactions, improved biodegradability, and a low waste profile in the body. Toward such sophistication in design aspects, the current state of the field focuses on exploiting and engineering physical and chemical properties of materials to encode and program intelligence at the microscale. This requires an extensive multidisciplinary experience and expertise in materials science, chemistry, physics, medicinal biology, and engineering. Fostering multidisciplinary research over the past decade has tremendously contributed to the creation of a variety of micromotors and microswimmers. Nevertheless, a few studies have so far focused on sensing capabilities and adaptation of microrobots to the changes in the environment, which constitute the next direction in the field.[116,117,128]

On-board actuated and powered microrobots operate in far-from-equilibrium states, which requires a continuous supply of energy to maintain their activities for extended periods. To tackle a similar problem, biological organisms have evolved dynamic sensing and regulatory systems that impart precision, robustness, and versatility in the execution of intra- and intercellular tasks.[163] Similarly functioning artificial control pathways, developed for microrobots, would enable dynamic regulation and decision-making processes, such as fuel consumption rate, adjustment of the swimming speed, 3D localization, and functional engagements at the target body sites. Such a closed-loop control system at the microscale has not been available yet. Systems characterized as far from equilibrium can further allow a series of novel behaviors that are not attainable at equilibrium, such as swarming and the emergence of other collective properties.[164] Such behavior was covered briefly in the earlier sections, as only a limited number of studies has so far addressed the operations of microrobots in team or swarm organizations. Nevertheless, it is an important direction to take toward bioengineering applications in the form of parallel and distributed operations, depending on the scale and the type of the intervention.

Due to the abovementioned challenges of on-board microrobot designs, the first-generation microrobots developed by the off-board approach are closer to clinical, *in vivo* and lab-on-a-chip applications. In the off-board systems, wireless powering and guidance of microrobots eliminate the need for local fuel concerns, autonomous sensing and navigation toward the target site. To this end, however, more sophisticated and high-performance control systems need to be developed. This includes powering microrobots in deep regions inside the body without local heating, simultaneous imaging, actuation, and tracking of the physiological environment and the microrobot(s) during a given biomedical operation, and selectively addressing individual microrobots among a group.

Use of microrobots for lab-on-a-chip applications is another appealing near-term route, because of powerful micromanipulation and precisely controlled mobile tools provided

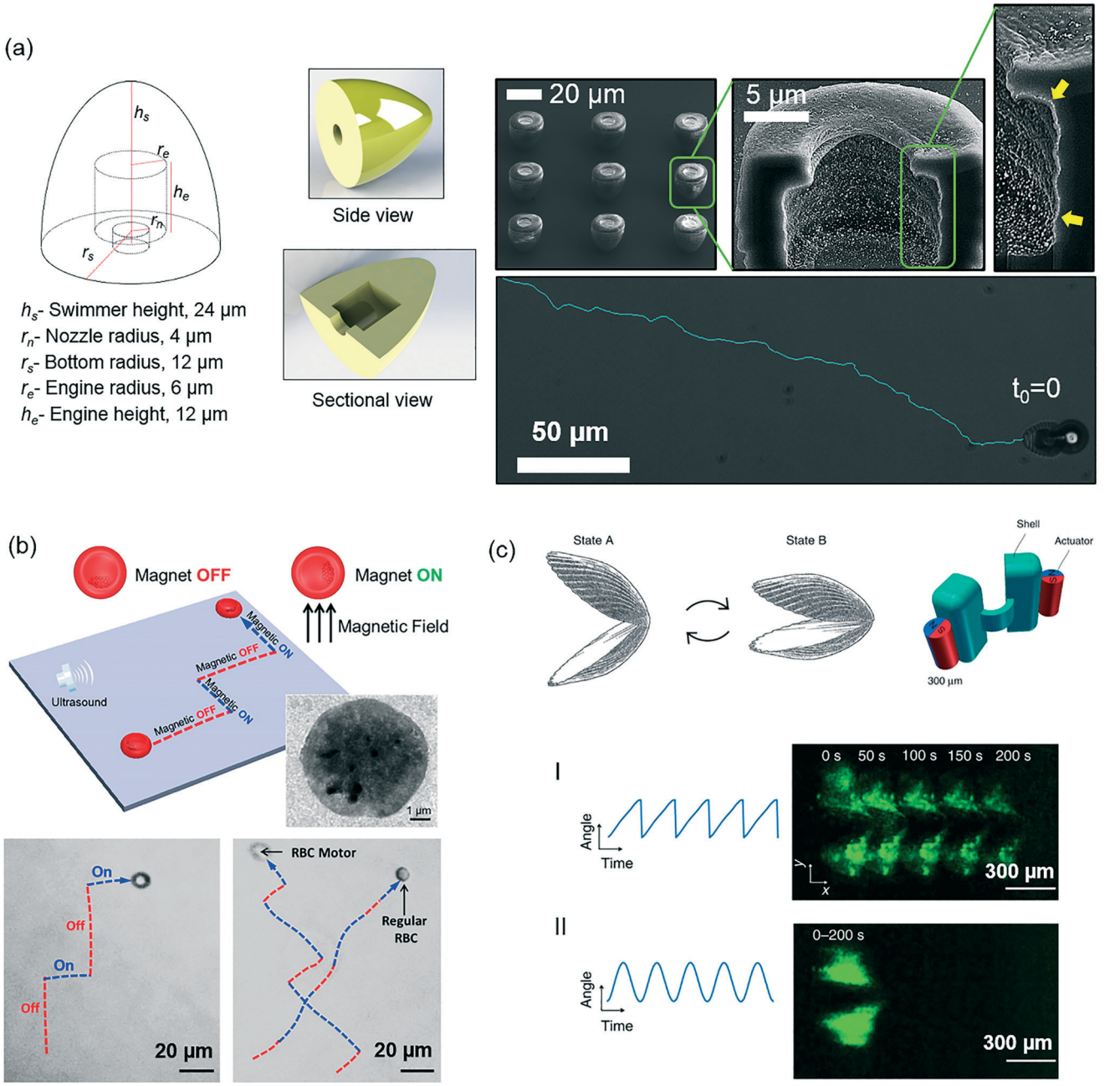

Fig. 5 Some of the critical future considerations in microrobotics concerning fabrication, materials, and design aspects. (a) CAD-designed and 3D-microprinted microrobots with patterned chemical regions can enable encoding complex microrobotic tasks and functions (reprinted with permission from ref. 166. Copyright 2017 from John Wiley & Sons, Inc.). (b) Red blood cells represent a rich source of making massive numbers of microrobots that are immunogenically safe and patient-specific for targeted cargo delivery applications (reprinted with permission from ref. 167. Copyright 2014 from the American Chemical Society). (c) Designing microrobot mobility components that are efficiently propelling in the complex viscoelastic physiological environment is central. The current designs that are typically optimized to operate in Newtonian fluids, *e.g.*, water, may need revisiting for *in vitro* and *in vivo* scenarios, especially taking the particular body location and local properties of the physiological fluid into account (reprinted with permission from ref. 169. Copyright 2014 from Nature Publishing Group).

at a size scale that can non-invasively access to small spaces. For example, individual cells or cell packs organized in unit tissue scaffolds could be assembled by means of a off-board powered microrobot for obtaining 3D heterogeneous tissue-mimetic constructs.[2] Particularly, the assembly of 3D parts, which require orientation and positional control, would be best addressed using microrobotic assembly. Handling small objects in very small fluid volumes for manipulation, moving and reconfiguring the components by means of 3D micro robots could make this route highly attractive for organ-on-a-chip applications where complex cellular materials with 3D microscale compositional features are positioned.

Fabrication of microrobots, in both on-board and off-board approaches, presents unique challenges concerning

design, fabrication process, and encoding operational capabilities. Conventional microfabrication techniques usually provide relatively simple geometric structures, such as tubes, spheres, and surfaces, with limited design flexibility and function. For example, a bubble-propelled micromotor requires well-compartmentalized placement of the catalyst and effective ejection of the jet bubbles in order to produce efficient propulsion from the catalytic reaction. On the other hand, realization of complex designs with programmable distribution of the catalyst and other functional components is a daunting task at the microscale. For this reason, the majority of the bubble-driven microswimmers are in the form of tubes, made with either electrodeposition or rolled up polymer films, and the catalyst is homogenously present everywhere located in the innermost layer.[165] Besides, because the propulsion in the low Reynolds regime suffers greatly from the viscous drag, an optimal 3D microswimmer body design is an important parameter to achieve the maximum propulsion efficiencies.

Integration of computer-aided design (CAD) to microfabrication technologies has been a significant advancement to realize sophisticated 3D designs that could not be conceivable with the existing methods. To this end, application of additive manufacturing processes enabled by two-photon crosslinking, also known as direct laser writing technology, has opened up an unprecedented 3D design and manufacturing freedom at the microscale. In regard to its microrobotic applications, Servant *et al.* used this technology to develop cork-screw-type magnetic microswimmers.[70] Very recently, Ceylan *et al.* has advanced this technology by adding chemical versatility to the 3D-printed bodies, and thereby realizing the first computer-designed and low drag bubble-propelled microswimmers (Fig. 5a).[166] Tailorable local 3D chemical properties would allow advanced programmable functionalities, and hence could lead to novel design opportunities for microrobots.

Material biocompatibility is an important aspect for devices to operate in the living environment. This has attracted little attention so far, while accumulating knowledge and expertise in tissue engineering and related disciplines could provide a wealth of inspirations regarding type and composition of the materials for fabrication of microrobots. When a microrobot is inside biological fluids it is prone to attacks by the cells of immune system, and its circulation time is closely related with the time of recognition by the host immune system. A possible approach could be the use of patient's own biomaterials to fabricate the microrobot bodies. Such a personalized solution could largely circumvent the immune response, as the body would recognize the microrobots as self. For example, turning natural red blood cells into functional micromotors by loading them with magnetic nanoparticles is a promising example toward this purpose (Fig. 5b).[167] Wu *et al.* developed such systems, and could propel them by ultrasound and guide them by magnetic fields. These cells are vastly available in the blood, as such 2.4 million of those cells are being produced each second.[168] Use of red blood cells as the base material could be interesting and useful to enable massive amounts of microrobots that could be hardly achieved by any of the existing microfabrication technologies. Moreover, they are mechanically robust and can change shape under applied stress without undergoing plastic deformation. They have an average of 120 days lifetime, during which they travel around 400 km.[168] Design systems based on red blood cells could therefore greatly help robust locomotion in blood vessels by dynamically adjusting their diameters.

In the earlier sections, we emphasized the importance of non-reciprocal motion in the low Reynolds numbers for a microswimmer to propel. However, most biological fluids are non-Newtonian, and thereby exhibiting viscoelastic behavior. This environment is vastly different from what the scallop theory was based upon, *i.e.*, Newtonian fluids. Qiu *et al.* realized that a microswimmer can also move with reciprocal periodic body-shape changes in non-Newtonian fluids (Fig. 5c).[169] The net propulsion here is caused by the modulation of the local fluid viscosity by varying the shear rate exerted by the swimmer body itself. This demonstration opens new design considerations for microrobots that are built to operate in non-Newtonian physiological fluids. Moreover, the existing microswimmers may need to be revisited for their optimal design and performance in the living environment, in which their propulsion speed, energy efficiency, and control may significantly vary.

Glossary

Microrobot	A reprogrammable, microscopic machine with partly or fully self-contained capabilities entitled by on-board motion, perception, and learning.
Micromotor	A component of microrobot that can convert energy from various sources, such as magnetic fields, light, or chemical bonds, to do mechanical work in the form of directional motion.
Microswimmer	A specific locomotion mode of a microrobot that is able to propel and do directional motion in bulk fluid.
Off-board approach	Remotely actuated, powered, and steered microrobots.
On-board approach	A microrobot is self-contained with all the components necessary to move, sense, and operate in a manner independent from an external intervention.
Biohybrid design	Single-celled microrganisms are physically incorporated with synthetic materials to exploit cells' integrated powering, motility, and sensing capabilities.
Fuel	Chemical that is consumed by the micromotor to produce thrust force.

Functional component	Components of a microrobot apart from its mobility, such as drug cargo, gripper, controlled release system, and sensing.

Acknowledgements

The authors acknowledge funding from the Max Planck Society and the Max Planck ETH Center for Learning Systems. M. S. was partially supported by National Science Foundation National Robotics Initiative Program Grant 1317477. Open Access funding provided by the Max Planck Society.

References

1 M. Medina-Sánchez, L. Schwarz, A. K. Meyer, F. Hebenstreit and O. G. Schmidt, *Nano Lett.*, 2016, **16**, 555–561.
2 S. Tasoglu, E. Diller, S. Guven, M. Sitti and U. Demirci, *Nat. Commun.*, 2014, **5**, 3124.
3 W. B. Rogers, W. M. Shih and V. N. Manoharan, *Nat. Rev. Mater.*, 2016, **1**, 16008.
4 J. Yan, M. Han, J. Zhang, C. Xu, E. Luijten and S. Granick, *Nat. Mater.*, 2016, **15**, 1095–1099.
5 S. Palagi, A. G. Mark, S. Y. Reigh, K. Melde, T. Qiu, H. Zeng, C. Parmeggiani, D. Martella, A. Sanchez-Castillo, N. Kapernaum, F. Giesselmann, D. S. Wiersma, E. Lauga and P. Fischer, *Nat. Mater.*, 2016, **15**, 647–653.
6 M. Sitti, H. Ceylan, W. Hu, J. Giltinan, M. Turan, S. Yim and E. Diller, *Proc. IEEE*, 2015, **103**, 205–224.
7 M. Sitti, *Nature*, 2009, **458**, 1121–1122.
8 M. P. Kummer, J. J. Abbott, B. E. Kratochvil, R. Borer, A. Sengul and B. J. Nelson, *IEEE Trans. Robot.*, 2010, **26**, 1006–1017.
9 J. Pokki, O. Ergeneman, S. Sevim, V. Enzmann, H. Torun and B. J. Nelson, *Biomed. Microdevices*, 2015, **17**, 1–9.
10 B. J. Nelson, I. K. Kaliakatsos and J. J. Abbott, *Annu. Rev. Biomed. Eng.*, 2010, **12**, 55–85.
11 J. Giltinan, E. Diller and M. Sitti, *Lab Chip*, 2016, **16**, 4445–4457.
12 S. E. Chung, X. Dong and M. Sitti, *Lab Chip*, 2015, **15**, 1667–1676.
13 A. K. Capulli, K. Tian, N. Mehandru, A. Bukhta, S. F. Choudhury, M. Suchyta and K. K. Parker, *Lab Chip*, 2014, **14**, 3181–3186.
14 J. Li and D. J. Mooney, *Nat. Rev. Mater.*, 2016, **1**, 16071.
15 J. Cohen, *Science*, 1995, **270**, 908–908.
16 G. W. Ashley, J. Henise, R. Reid and D. V. Santi, *Proc. Natl. Acad. Sci. U. S. A.*, 2013, **110**, 2318–2323.
17 E. Diller and M. Sitti, *Foundations and Trends in Robotics*, 2013, **2**, 143–259.
18 M. Sitti, *IEEE Robot. Autom. Mag.*, 2007, **14**, 53–60.
19 E. M. Purcell, *Am. J. Phys.*, 1977, **45**, 3–11.
20 D. B. Dusenbery, *Living at the Microscale*, Harvard University Press, 2009.
21 D. Schamel, A. G. Mark, J. G. Gibbs, C. Miksch, K. I. Morozov, A. M. Leshansky and P. Fischer, *ACS Nano*, 2014, **8**, 8794–8801.
22 M. Alarcón-Correa, D. Walker, T. Qiu and P. Fischer, *Eur. Phys. J.: Spec. Top.*, 2016, **225**, 2241–2254.
23 K. Kim, J. Guo, Z. X. Liang, F. Q. Zhu and D. L. Fan, *Nanoscale*, 2016, **8**, 10471–10490.
24 C. R. Reid, H. MacDonald, R. P. Mann, J. A. R. Marshall, T. Latty and S. Garnier, *J. R. Soc., Interface*, 2016, **13**, 20160030.
25 P. C. Marijuán, J. Navarro and R. del Moral, *Biosystems*, 2010, **99**, 94–103.
26 F. Cvrčková, H. Lipavská and V. Žárský, *Plant Signaling Behav.*, 2009, **4**, 394–399.
27 R. W. Carlsen and M. Sitti, *Small*, 2014, **10**, 3831–3851.
28 A. W. Feinberg, *Annu. Rev. Biomed. Eng.*, 2015, **17**, 243–265.
29 M. P. Kummer, J. J. Abbott, B. E. Kratochvil, R. Borer, A. Sengul and B. J. Nelson, *IEEE Trans. Robot.*, 2010, **26**, 1006–1017.
30 D. C. Meeker, E. H. Maslen, R. C. Ritter and F. M. Creighton, *IEEE Trans. Magn.*, 1996, **32**, 320–328.
31 T. Honda, K. I. Arai and K. Ishiyama, *IEEE Trans. Magn.*, 1996, **32**, 5085–5087.
32 J. F. Schenck, *J. Magn. Reson. Imaging*, 2000, **12**, 2–19.
33 *Criteria for significant risk investigations of magnetic resonance diagnostic devices*, U.S. Food and Drug Administeration, 2003.
34 A. M. Maier, C. Weig, P. Oswald, E. Frey, P. Fischer and T. Liedl, *Nano Lett.*, 2016, **16**, 906–910.
35 R. Dreyfus, J. Baudry, M. L. Roper, M. Fermigier, H. A. Stone and J. Bibette, *Nature*, 2005, **437**, 862–865.
36 J. Zhang and E. Diller, *IEEE International Conference on Intelligent Robots and Systems*, 2015, pp. 1706–1711.
37 J. Zhang, P. Jain and E. Diller, *IEEE International Conference on Robotics and Automation (ICRA)*, 2016, pp. 1933–1938.
38 Z. Ye, S. Régnier and M. Sitti, *IEEE Trans. Robot.*, 2014, **30**, 3–13.
39 I. S. Khalil, A. F. Tabak, K. Sadek, D. Mahdy, N. Hamdi and M. Sitti, *IEEE Robot. Autom. Lett.*, 2017, **2**, 927–934.
40 I. S. Khalil, A. F. Tabak, A. Klingner and M. Sitti, *Appl. Phys. Lett.*, 2016, **109**, 033701.
41 I. S. Khalil, K. Youakim, A. Sánchez and S. Misra, *IEEE/RSJ International Conference on Intelligent Robots and Systems*, 2016, pp. 4686–4691.
42 G. Z. Lum, Z. Ye, X. Dong, H. Marvi, O. Erin, W. Hu and M. Sitti, *Proc. Natl. Acad. Sci. U. S. A.*, 2016, **113**, E6007.
43 J. M. den Toonder and P. R. Onck, *Trends Biotechnol.*, 2013, **31**, 85–91.
44 P. J. Vach, P. Fratzl, S. Klumpp and D. Faivre, *Nano Lett.*, 2015, **15**, 7064–7070.
45 P. J. Vach and D. Faivre, *Sci. Rep.*, 2015, **5**, 9364.
46 E. Diller, J. Giltinan, G. Z. Lum, Z. Ye and M. Sitti, *Int. J. Rob. Res.*, 2016, **35**, 114.
47 P. Ryan and E. Diller, *IEEE International Conference on Robotics and Automation (ICRA)*, 2016, pp. 1731–1736.
48 G. Go, H. Choi, S. Jeong, C. Lee, S. Y. Ko, J.-O. Park and S. Park, *IEEE Trans. Magn.*, 2015, **51**, 1–7.
49 F. Qiu, S. Fujita, R. Mhanna, L. Zhang, B. R. Simona and B. J. Nelson, *Adv. Funct. Mater.*, 2015, **25**, 1666–1671.
50 M. Hoop, Y. Shen, X. Z. Chen, F. Mushtaq, L. M. Iuliano, M. S. Sakar, A. Petruska, M. J. Loessner, B. J. Nelson and S. Pané, *Adv. Funct. Mater.*, 2015, **26**, 1063–1069.

51 P. W. Egolf, N. Shamsudhin, S. Pané, D. Vuarnoz, J. Pokki, A.-G. Pawlowski, P. Tsague, B. de Marco, W. Bovy and S. Tucev, *J. Appl. Phys.*, 2016, **120**, 064304.
52 C. Chen, L. Chen, Y. Yi, C. Chen, L.-F. Wu and T. Song, *Appl. Environ. Microbiol.*, 2016, **82**, 2219–2226.
53 D. Walker, B. T. Käsdorf, H.-H. Jeong, O. Lieleg and P. Fischer, *Sci. Adv.*, 2015, **1**, e1500501.
54 Z. Ye and M. Sitti, *Lab Chip*, 2014, **14**, 2177–2182.
55 Y. Ding, F. Qiu, X. Casadevall i Solvas, F. W. Y. Chiu, B. J. Nelson and A. deMello, *Micromachines*, 2016, **7**, 25.
56 T.-Y. Huang, F. Qiu, H.-W. Tung, X.-B. Chen, B. J. Nelson and M. S. Sakar, *Appl. Phys. Lett.*, 2014, **105**, 114102.
57 T.-Y. Huang, F. Qiu, H.-W. Tung, K. E. Peyer, N. Shamsudhin, J. Pokki, L. Zhang, X.-B. Chen, B. J. Nelson and M. S. Sakar, *RSC Adv.*, 2014, **4**, 26771–26771.
58 E. Diller and M. Sitti, *Adv. Funct. Mater.*, 2014, **24**, 4397–4404.
59 W. Zhu, J. Li, Y. J. Leong, I. Rozen, X. Qu, R. Dong, Z. Wu, W. Gao, P. H. Chung, J. Wang and S. Chen, *Adv. Mater.*, 2015, **27**, 4411–4417.
60 Z. Wu, B. E.-F. de Ávila, A. Martín, C. Christianson, W. Gao, S. K. Thamphiwatana, A. Escarpa, Q. He, L. Zhang and J. Wang, *Nanoscale*, 2015, **7**, 13680–13686.
61 J. Feng, J. Yuan and S. K. Cho, *Lab Chip*, 2016, **16**, 2317–2325.
62 J. Feng, J. Yuan and S. K. Cho, *Lab Chip*, 2015, **15**, 1554–1562.
63 J. O. Kwon, J. S. Yang, J. B. Chae and S. K. Chung, *Sens. Actuators, A*, 2014, **215**, 77–82.
64 I. S. Park, J. H. Shin, Y. R. Lee and S. K. Chung, *Sens. Actuators, A*, 2016, **248**, 214–222.
65 Q. Chao, J. Yu, C. Dai, T. Xu, L. Zhang, C. C. Wang and X. Jin, *IEEE Int. Conf. Robot. Autom.*, 2016, 5230–5235.
66 M. Salehizadeh and E. Diller, *Journal of Micro-Bio Robotics*, 2017, DOI: 10.1007/s12213-017-0095-5.
67 D. Wong, E. B. Steager and V. Kumar, *IEEE Robot. Autom. Lett.*, 2016, **1**, 554–561.
68 S. Chowdhury, W. Jing and D. J. Cappelleri, *Micromachines*, 2015, **7**, 3.
69 G. Go, H. Choi, S. Jeong, S. Y. Ko, J.-O. Park and S. Park, *Smart Mater. Struct.*, 2016, **25**, 035004.
70 A. Servant, F. Qiu, M. Mazza, K. Kostarelos and B. J. Nelson, *Adv. Mater.*, 2015, **27**, 2981–2988.
71 S. Jeong, H. Choi, G. Go, C. Lee, K. S. Lim, D. S. Sim, M. H. Jeong, S. Y. Ko, J.-O. Park and S. Park, *Med. Eng. Phys.*, 2016, **38**, 403–410.
72 J. Pokki, J. Parmar, O. Ergeneman, H. Torun, M. Guerrero, E. Pellicer, J. Sort, S. Pané and B. J. Nelson, *ACS Appl. Mater. Interfaces*, 2015, **7**, 22018–22028.
73 O. Felfoul, A. Becker, C. Bergeles and P. E. Dupont, *IEEE Trans. Robot*, 2015, **31**, 387–399.
74 O. Felfoul, A. T. Becker, G. Fagogenis and P. E. Dupont, *Sci. Rep.*, 2016, **6**, 33567.
75 A. T. Becker, O. Felfoul and P. E. Dupont, *IEEE International Conference on Robotics and Automation (ICRA)*, 2015, pp. 1184–1189.
76 N. Olamaei, F. Cheriet, S. Deschênes and S. Martel, *Appl. Phys. Lett.*, 2014, **104**, 213703.
77 A. Sharafi, N. Olamaei and S. Martel, *Journal of Micro-Bio Robotics*, 2015, **10**, 27–35.
78 M. Latulippe, O. Felfoul, P. E. Dupont and S. Martel, *Appl. Phys. Lett.*, 2016, **108**, 062403.
79 M. Latulippe and S. Martel, *IEEE Trans. Robot.*, 2015, **31**, 1353–1363.
80 P. Chen, S. Güven, O. B. Usta, M. L. Yarmush and U. Demirci, *Adv. Healthcare Mater.*, 2015, **4**, 1937–1943.
81 C. Bouyer, P. Chen, S. Güven, T. T. Demirtaş, T. J. F. Nieland, F. Padilla and U. Demirci, *Adv. Mater.*, 2016, **28**, 161–167.
82 S. Li, P. Glynne-Jones, O. G. Andriotis, K. Y. Ching, U. S. Jonnalagadda, R. O. C. Oreffo, M. Hill and R. S. Tare, *Lab Chip*, 2014, **14**, 4475–4485.
83 D. Ahmed, M. Lu, A. Nourhani, P. E. Lammert, Z. Stratton, H. S. Muddana, V. H. Crespi and T. J. Huang, *Sci. Rep.*, 2015, **5**, 9744.
84 D. Ahmed, T. Baasch, B. Jang, S. Pane, J. Dual and B. J. Nelson, *Nano Lett.*, 2016, **16**, 4968–4974.
85 M. Kaynak, A. Ozcelik, A. Nourhani, P. E. Lammert, V. H. Crespi and T. J. Huang, *Lab Chip*, 2017, **17**(3), 395–400.
86 J. Wu, *J. Acoust. Soc. Am.*, 1991, **89**, 2140–2143.
87 F. Soto, A. Martin, S. Ibsen, M. Vaidyanathan, V. Garcia-Gradilla, Y. Levin, A. Escarpa, S. C. Esener and J. Wang, *ACS Nano*, 2016, **10**, 1522–1528.
88 T. Qiu, S. Palagi, A. G. Mark, K. Melde, F. Adams and P. Fischer, *Appl. Phys. Lett.*, 2016, **109**, 191602.
89 K. Melde, A. G. Mark, T. Qiu and P. Fischer, *Nature*, 2016, **537**, 518–522.
90 A. Karbalaei, R. Kumar and H. J. Cho, *Micromachines*, 2016, **7**, 13.
91 M. A. Rahman, J. Cheng and A. T. Ohta, *IEEE 11th Annual International Conference on Nano/Micro Engineered and Molecular Systems (NEMS)*, 2016, pp. 279–282.
92 N. Takahashi, Z. Wang, M. A. Rahman, J. Cheng and A. T. Ohta, *IEEE 11th Annual International Conference on Nano/Micro Engineered and Molecular Systems (NEMS)*, 2016, pp. 237–240.
93 N. Bjelobrk, H.-L. Girard, S. B. Subramanyam, H.-M. Kwon, D. Quéré and K. K. Varanasi, *Phys. Rev. Fluids*, 2016, **1**, 063902.
94 L. Zhang, H. Zhang, M. Liu and B. Dong, *ACS Appl. Mater. Interfaces*, 2016, **8**(24), 15654–15660.
95 S. Palagi, A. G. Mark, S. Y. Reigh, K. Melde, T. Qiu, H. Zeng, C. Parmeggiani, D. Martella, A. Sanchez-Castillo and N. Kapernaum, *Nat. Mater.*, 2016, **15**(6), 647–653.
96 H. Zeng, P. Wasylczyk, C. Parmeggiani, D. Martella, M. Burresi and D. S. Wiersma, *Adv. Mater.*, 2015, **27**, 3883–3887.
97 M. Rogóż, H. Zeng, C. Xuan, D. S. Wiersma and P. Wasylczyk, *Adv. Opt. Mater.*, 2016, **4**, 1689–1694.
98 K. C. Neuman and S. M. Block, *Rev. Sci. Instrum.*, 2004, **75**, 2787–2809.
99 O. Ilic, I. Kaminer, Y. Lahini, H. Buljan and M. Soljačić, *ACS Photonics*, 2016, **3**, 197–202.

100 M. J. Villangca, D. Palima, A. R. Bañas and J. Glückstad, *Light: Sci. Appl.*, 2016, **5**, e16148.
101 A. Miniewicz, S. Bartkiewicz, H. Orlikowska and K. Dradrach, *Sci. Rep.*, 2016, **6**, 34787.
102 J. Li, I. Rozen and J. Wang, *ACS Nano*, 2016, **10**, 5619–5634.
103 L. K. E. A. Abdelmohsen, M. Nijemeisland, G. M. Pawar, G.-J. A. Janssen, R. J. M. Nolte, J. C. M. van Hest and D. A. Wilson, *ACS Nano*, 2016, **10**, 2652–2660.
104 X. Ma, S. Jang, M. N. Popescu, W. E. Uspal, A. Miguel-López, K. Hahn, D.-P. Kim and S. Sánchez, *ACS Nano*, 2016, **10**, 8751–8759.
105 X. Ma, A. Jannasch, U.-R. Albrecht, K. Hahn, A. Miguel-López, E. Schäffer and S. Sánchez, *Nano Lett.*, 2015, **15**, 7043–7050.
106 X. Ma, K. Hahn and S. Sanchez, *J. Am. Chem. Soc.*, 2015, **137**, 4976–4979.
107 S. Sengupta, K. K. Dey, H. S. Muddana, T. Tabouillot, M. E. Ibele, P. J. Butler and A. Sen, *J. Am. Chem. Soc.*, 2013, **135**, 1406–1414.
108 X. Ma, A. C. Hortelão, T. Patiño and S. Sánchez, *ACS Nano*, 2016, **10**(10), 9111–9122.
109 J. G. Gibbs and Y.-P. Zhao, *Appl. Phys. Lett.*, 2009, **94**, 163104.
110 J. G. S. Moo and M. Pumera, *Chem. – Eur. J.*, 2015, **21**, 58–72.
111 S. Ebbens, D. A. Gregory, G. Dunderdale, J. R. Howse, Y. Ibrahim, T. B. Liverpool and R. Golestanian, *EPL*, 2014, **106**, 58003.
112 A. Brown and W. Poon, *Soft Matter*, 2014, **10**, 4016–4027.
113 C. Bechinger, R. Di Leonardo, H. Löwen, C. Reichhardt, G. Volpe and G. Volpe, *Rev. Mod. Phys.*, 2016, **88**, 045006.
114 J. Li, G. Huang, M. Ye, M. Li, R. Liu and Y. Mei, *Nanoscale*, 2011, **3**, 5083–5089.
115 T. Xu, F. Soto, W. Gao, V. Garcia-Gradilla, J. Li, X. Zhang and J. Wang, *J. Am. Chem. Soc.*, 2014, **136**, 8552–8555.
116 V. Magdanz, G. Stoychev, L. Ionov, S. Sanchez and O. G. Schmidt, *Angew. Chem.*, 2014, **126**, 2711–2715.
117 Y. Tu, F. Peng, X. Sui, Y. Men, P. B. White, J. C. M. van Hest and D. A. Wilson, *Nat. Chem.*, 2017, **9**, 480–486.
118 F. Mou, Y. Li, C. Chen, W. Li, Y. Yin, H. Ma and J. Guan, *Small*, 2015, **11**, 2564–2570.
119 M. Guix, C. C. Mayorga-Martinez and A. Merkoçi, *Chem. Rev.*, 2014, **114**, 6285–6322.
120 F. Peng, Y. Tu, J. C. M. van Hest and D. A. Wilson, *Angew. Chem., Int. Ed.*, 2015, **54**, 11662–11665.
121 J. Parmar, D. Vilela, E. Pellicer, D. Esqué-de los Ojos, J. Sort and S. Sánchez, *Adv. Funct. Mater.*, 2016, **26**, 4152–4161.
122 D. A. Gregory, Y. Zhang, P. J. Smith, X. Zhao and S. J. Ebbens, *Small*, 2016, **12**, 4048–4055.
123 J. Li, V. V. Singh, S. Sattayasamitsathit, J. Orozco, K. Kaufmann, R. Dong, W. Gao, B. Jurado-Sanchez, Y. Fedorak and J. Wang, *ACS Nano*, 2014, **8**, 11118–11125.
124 Z. Wu, J. Li, B. E.-F. de Ávila, T. Li, W. Gao, Q. He, L. Zhang and J. Wang, *Adv. Funct. Mater.*, 2015, **25**, 7497–7501.
125 W. Gao, R. Dong, S. Thamphiwatana, J. Li, W. Gao, L. Zhang and J. Wang, *ACS Nano*, 2015, **9**, 117–123.
126 C. Chen, E. Karshalev, J. Li, F. Soto, R. Castillo, I. Campos, F. Mou, J. Guan and J. Wang, *ACS Nano*, 2016, **10**, 10389–10396.
127 J. Li, S. Thamphiwatana, W. Liu, B. Esteban-Fernández de Ávila, P. Angsantikul, E. Sandraz, J. Wang, T. Xu, F. Soto, V. Ramez, X. Wang, W. Gao, L. Zhang and J. Wang, *ACS Nano*, 2016, **10**, 9536–9542.
128 M. Nijemeisland, L. K. E. A. Abdelmohsen, W. T. S. Huck, D. A. Wilson and J. C. M. van Hest, *ACS Cent. Sci.*, 2016, **2**, 843–849.
129 U. Choudhury, L. Soler, J. G. Gibbs, S. Sanchez and P. Fischer, *Chem. Commun.*, 2015, **51**, 8660–8663.
130 J. R. Howse, R. A. L. Jones, A. J. Ryan, T. Gough, R. Vafabakhsh and R. Golestanian, *Phys. Rev. Lett.*, 2007, **99**, 048102.
131 X. Ma, X. Wang, K. Hahn and S. Sánchez, *ACS Nano*, 2016, **10**, 3597–3605.
132 X. Ma and S. Sanchez, *Chem. Commun.*, 2015, **51**, 5467–5470.
133 B. ten Hagen, F. Kümmel, R. Wittkowski, D. Takagi, H. Löwen and C. Bechinger, *Nat. Commun.*, 2014, **5**, 4829.
134 W. E. Uspal, M. N. Popescu, S. Dietrich and M. Tasinkevych, *Soft Matter*, 2015, **11**, 434–438.
135 F. Yang, S. Qian, Y. Zhao and R. Qiao, *Langmuir*, 2016, **32**, 5580–5592.
136 J. Simmchen, J. Katuri, W. E. Uspal, M. N. Popescu, M. Tasinkevych and S. Sánchez, *Nat. Commun.*, 2016, **7**, 10598.
137 Z. Hosseinidoust, B. Mostaghaci, O. Yasa, B.-W. Park, A. V. Singh and M. Sitti, *Adv. Drug Delivery Rev.*, 2016, **106**, 27–44.
138 J. Xi, J. J. Schmidt and C. D. Montemagno, *Nat. Mater.*, 2005, **4**, 180–184.
139 M. P. Hughes and H. Morgan, *Biotechnol. Prog.*, 1999, **15**, 245–249.
140 D. P. L. Green, *Biol. Rev.*, 1988, **63**, 79–105.
141 A. V. Singh and M. Sitti, *Adv. Healthcare Mater.*, 2016, **5**, 2325–2331.
142 Q. Ma, C. Chen, S. Wei, C. Chen, L.-F. Wu and T. Song, *Biomicrofluidics*, 2012, **6**, 024107.
143 E. B. Steager, M. S. Sakar, D. H. Kim, V. Kumar, G. J. Pappas and M. J. Kim, *J. Micromech. Microeng.*, 2011, **21**, 035001.
144 J. Zhuang and M. Sitti, *Sci. Rep.*, 2016, **6**, 32135.
145 R. W. Carlsen, M. R. Edwards, J. Zhuang, C. Pacoret and M. Sitti, *Lab Chip*, 2014, **14**, 3850–3859.
146 J. B. Mathieu and S. Martel, *Magn. Reson. Med.*, 2010, **63**, 1336–1345.
147 P. Pouponneau, J.-C. Leroux and S. Martel, *Biomaterials*, 2009, **30**, 6327–6332.
148 J. Zhuang, R. W. Carlsen and M. Sitti, *Sci. Rep.*, 2015, **5**, 11403.
149 B. Hu and Y. Tu, *PLoS Comput. Biol.*, 2014, **10**, e1003672.
150 J.-W. Han, Y. J. Choi, S. Cho, S. Zheng, S. Y. Ko, J.-O. Park and S. Park, *Sens. Actuators, B*, 2016, **224**, 217–224.

151 M. Zhao, M. Yang, X.-M. Li, P. Jiang, E. Baranov, S. Li, M. Xu, S. Penman and R. M. Hoffman, *Proc. Natl. Acad. Sci. U. S. A.*, 2005, **102**, 755–760.
152 O. Felfoul, M. Mohammadi, S. Taherkhani, D. de Lanauze, Y. Z. Xu, D. Loghin, S. Essa, S. Jancik, D. Houle and M. Lafleur, *Nat. Nanotechnol.*, 2016, **11**, 941–947.
153 I. S. Khalil, V. Magdanz, S. Sanchez, O. G. Schmidt and S. Misra, *Journal of Micro-Bio Robotics*, 2014, **9**, 79–86.
154 V. Magdanz, S. Sanchez and O. G. Schmidt, *Adv. Mater.*, 2013, **25**, 6581–6588.
155 V. Magdanz, M. Guix, F. Hebenstreit and O. G. Schmidt, *Adv. Mater.*, 2016, **28**, 4084–4089.
156 H. Kim and M. J. Kim, *IEEE Trans. Robot.*, 2016, **32**, 125–137.
157 R. Raman, C. Cvetkovic, S. G. M. Uzel, R. J. Platt, P. Sengupta, R. D. Kamm and R. Bashir, *Proc. Natl. Acad. Sci. U. S. A.*, 2016, **113**, 3497–3502.
158 S.-J. Park, M. Gazzola, K. S. Park, S. Park, V. Di Santo, E. L. Blevins, J. U. Lind, P. H. Campbell, S. Dauth, A. K. Capulli, F. S. Pasqualini, S. Ahn, A. Cho, H. Yuan, B. M. Maoz, R. Vijaykumar, J.-W. Choi, K. Deisseroth, G. V. Lauder, L. Mahadevan and K. K. Parker, *Science*, 2016, **353**, 158.
159 T. Bruegmann, T. van Bremen, C. C. Vogt, T. Send, B. K. Fleischmann and P. Sasse, *Nat. Commun.*, 2015, **6**, 7153.
160 B. J. Williams, S. V. Anand, J. Rajagopalan and M. T. A. Saif, *Nat. Commun.*, 2014, **5**, 3081.
161 S. V. Anand, M. Yakut Ali and M. T. A. Saif, *Lab Chip*, 2015, **15**, 1879–1888.
162 C. Cvetkovic, R. Raman, V. Chan, B. J. Williams, M. Tolish, P. Bajaj, M. S. Sakar, H. H. Asada, M. T. A. Saif and R. Bashir, *Proc. Natl. Acad. Sci. U. S. A.*, 2014, **111**, 10125–10130.
163 M. Freeman, *Nature*, 2000, **408**, 313–319.
164 A. Bricard, J.-B. Caussin, N. Desreumaux, O. Dauchot and D. Bartolo, *Nature*, 2013, **503**, 95–98.
165 P. Jemish, M. Xing, K. Jaideep, S. Juliane, M. S. Morgan, T.-P. Carolina, S. Lluís and S. Samuel, *Sci. Technol. Adv. Mater.*, 2015, **16**, 014802.
166 H. Ceylan, I. C. Yasa and M. Sitti, *Adv. Mater.*, 2017, 1605072, DOI: 10.1002/adma.201605072.
167 Z. Wu, T. Li, J. Li, W. Gao, T. Xu, C. Christianson, W. Gao, M. Galarnyk, Q. He, L. Zhang and J. Wang, *ACS Nano*, 2014, **8**, 12041–12048.
168 E. Sackmann, *Handb. Biol. Phys.*, 1995, **1**, 1–63.
169 T. Qiu, T.-C. Lee, A. G. Mark, K. I. Morozov, R. Münster, O. Mierka, S. Turek, A. M. Leshansky and P. Fischer, *Nat. Commun.*, 2014, **5**, 5119.

